HHS Public Access

Author manuscript

Mol Cell Neurosci. Author manuscript; available in PMC 2018 January 01.

Published in final edited form as:

Mol Cell Neurosci. 2017 January ; 78: 9–24. doi:10.1016/j.mcn.2016.11.004.

Neurexin, Neuroligin and Wishful Thinking Coordinate Synaptic Cytoarchitecture and Growth at Neuromuscular Junctions

Swati Banerjee[*], **Anandakrishnan Venkatesan**, and **Manzoor A. Bhat**

Department of Physiology, School of Medicine, University of Texas Health Science Center, San Antonio, TX 78229-3900, USA

Abstract

Trans-synaptic interactions involving Neurexins and Neuroligins are thought to promote adhesive interactions for precise alignment of the pre- and postsynaptic compartments and organize synaptic macromolecular complexes across species. In *Drosophila*, while Neurexin (Dnrx) and Neuroligins (Dnlg) are emerging as central organizing molecules at synapses, very little is known of the spectrum of proteins that might be recruited to the Dnrx/Dnlg trans-synaptic interface for organization and growth of the synapses. Using full length and truncated forms of Dnrx and Dnlg1 together with cell biological analyses and genetic interactions, we report novel functions of Dnrx and Dnlg1 in clustering of pre- and postsynaptic proteins, coordination of synaptic growth and ultrastructural organization. We show that Dnrx and Dnlg1 extracellular and intracellular regions are required for proper synaptic growth and localization of Dnlg1 and Dnrx, respectively. *dnrx* and *dnlg1* single and double mutants display altered subcellular distribution of Discs large (Dlg), which is the homolog of mammalian post-synaptic density protein, PSD95. *dnrx* and *dnlg1* mutants also display ultrastructural defects ranging from abnormal active zones, misformed pre- and post-synaptic areas with underdeveloped subsynaptic reticulum. Interestingly, *dnrx* and *dnlg1* mutants have reduced levels of the BMP receptor Wishful thinking (Wit), and Dnrx and Dnlg1 are required for proper localization and stability of Wit. In addition, the synaptic overgrowth phenotype resulting from the overexpression of Dnrx fails to manifest in *wit* mutants. Phenotypic analyses of *dnrx/wit* and *dnlg1/wit* mutants indicate that Dnrx/Dnlg1/Wit coordinate synaptic growth and architecture at the NMJ. Our findings also demonstrate that loss of Dnrx and Dnlg1 leads to decreased levels of the BMP co-receptor, Thickveins and the downstream effector phosphorylated Mad at the NMJ synapses indicating that Dnrx/Dnlg1 regulate components of the BMP signaling pathway. Together our findings reveal that Dnrx/Dnlg are at the core of a highly orchestrated process that combines adhesive and signaling mechanisms to ensure proper synaptic organization and growth during NMJ development.

[*]**Address correspondence to:** Swati Banerjee, Ph.D., Department of Physiology, University of Texas Health Science Center, 7703 Floyd Curl Drive, San Antonio, TX 78229-3900, USA, banerjees@uthscsa.edu.

Conflict of Interest

The authors declare no conflict of interest.

Keywords

Neuromuscular Junctions; Synaptic Growth; Subsynaptic Reticulum; Neurexin; Neuroligin 1; Wishful Thinking

1. Introduction

Trans-synaptic adhesive mechanisms underlie the precise organization and alignment of pre- and postsynaptic compartments to allow proper transmission of nerve signals in neuronal circuits. Since their discovery more than two decades ago, two protein families, the Neurexins (Nrxs) and Neuroligins (Nlgs) (Ushkaryov et al. 1992; Ichtchenko et al. 1995) have been shown to function as adhesion molecules bridging the synaptic cleft. Nrxs and Nlgs have emerged as central organizing molecules with synaptogenic abilities in organizing pre- and postsynaptic protein complexes at synapses (Scheiffele et al. 2000; Zhang et al. 2015; Rothwell et al. 2014). These proteins are also implicated in the organization of excitatory glutamatergic and inhibitory GABAergic synapses in mammalian brain (Prange et al. 2004; Graf et al. 2004; Chih et al. 2005; Aoto et al. 2015). The functional properties of Nrxs and Nlgs are conserved, as the *Drosophila* homologs of Neurexin (Dnrx) and Neuroligin (Dnlg) also play critical roles in the assembly and maintenance of the glutamatergic synapses at the larval neuromuscular junctions (NMJ), as lack of either Dnrx or Dnlg shows a significant reduction in synaptic growth at the NMJ (Li et al., 2007; Banovic et al., 2010; Chen et al., 2012; Mozer and Sandstrom, 2012; Xing et al. 2014). Despite these studies, many key questions still remain to be addressed in the context of the *Drosophila* larval NMJ. These include understanding what other synaptic proteins interact with Dnrx/Dnlg1 or get recruited to the trans-synaptic interface to orchestrate adhesive interactions, signaling and coordination of synaptic growth and architecture.

One line of evidence in favor of Dnrx and Dnlg1 function in maintaining trans-synaptic adhesion came from the ultrastructural studies of mutant synaptic boutons at the larval NMJ. Loss of both Dnrx and Dnlg1 revealed ultrastructural synaptic phenotypes that manifested as presynaptic membrane detachments with a characteristic ruffling morphology, suggesting lack of proper adhesion between the pre- and postsynaptic membrane apposition (Li et al. 2007; Banovic et al. 2010). Surprisingly, loss-of-function mutants of *wishful thinking (wit)*, which is a key presynaptic receptor of the Bone Morphogenetic Protein (BMP) pathway, also displayed similar membrane detachment phenotypes in NMJ boutons in addition to a drastic reduction in synaptic growth (Aberle et al., 2002; Marques et al., 2002). Since the BMP pathway is well characterized in *Drosophila* for the regulation of synapse assembly, maintenance, and function (Aberle et al., 2002; Marques et al., 2002; McCabe et al., 2003; Berke et al., 2013), the phenotypic similarities in the synaptic growth and ultrastructure observed in *dnrx, dnlg1* and *wit* mutants prompted us to investigate whether these proteins may collectively function in common developmental programs to regulate synaptic structural organization and growth.

Here we report the phenotypic consequences of single and double mutant combinations of *dnrx, dnlg1* and *wit* on synaptic growth and architecture. Genetic and biochemical

interaction studies reveal that Dnrx and Dnlg1 function together in regulating synaptic growth and exist in a macromolecular complex. Rescue analysis involving full length and truncated extracellular (N-terminal) and cytoplasmic (C-terminal) regions of Dnrx and Dnlg1 reveal the requirement of both N- and C-terminal regions for synaptic clustering of one another as well as synaptic growth. Immunolocalization analysis suggests that presynaptic Dnrx and Wit are interdependent for their proper localization at the NMJ synapses. Interestingly, absence of either Dnrx or Dnlg1 drastically affects Wit stability, and *dnrx* and *dnlg1* display trans-heterozygous genetic interactions with *wit*. Ultrastructural analysis of single and double mutants of *dnrx, dnlg1* and *wit* reveal a wide range of pre- and postsynaptic differentiation defects in addition to synaptic membrane detachments. *dnrx* and *dnlg1* also display genetic interactions with *Mad*, a downstream effector of the BMP pathway, and the levels of phosphorylated Mad (pMad) and Type 1 BMP receptor, Thickveins (Tkv), showed marked reduction at *dnrx* and *dnlg1* mutant synapses. Together our studies indicate a functional coordination between trans-synaptic adhesion and synaptic signaling mechanisms during NMJ development.

2. Materials and Methods

2.1 Fly Stocks

The fly strains used in this study were isogenized w^{1118} *Canton-S* line (a gift from V. Budnik) used as the wild type control, $dnrx^{273}$, *Df(3R)5C1* (a deficiency that removes *dnrx), UAS-dnrx* (Li et al., 2007), *UAS-*$dnrx^{\Delta N}$, *UAS-*$dnrx^{\Delta C}$ (Tian et al., 2013), $dnlg1^{\Delta 46}$, *UAS-dnlg1* (Mozer and Sandstrom, 2012), *UAS-dnlg1-GFP, UAS-dnlg1-*$GFP^{\Delta C}$ and *UAS-dnlg1-*$GFP^{\Delta N}$ (Banovic et al. 2010), *UAS-wit* (a gift from M. O'Connor); wit^{A12}, wit^{B11} (Marques et al. 2002) and Mad^{237}, Mad^{12} (Merino et al. 2009; Rawson et al. 2003). All other fly stocks were obtained from Bloomington Stock Center, Indiana. All flies were maintained at 22°C, 50% humidity and with a 12-hour light/dark cycle. To avoid over-crowding, all fly lines for various phenotypic analyses were set up using 10 females and 5 males and transferred every 24 hours into fresh media.

2.2 Immunohistochemistry and Confocal Imaging

Wandering third-instar larvae from various genotypes were dissected and fixed in either Bouin's fixative or 4% paraformaldehyde for 15 minutes and processed as previously described (Chen et al., 2012). Dnrx signal at NMJ was enhanced using previously described protocols (Li et al., 2007). Confocal images of all genotypes of larvae belonging to the same experimental group were acquired using same settings with a Zeiss LSM710 confocal microscope and image editing was done using Adobe Photoshop.

The following primary antibodies were used: FITC-conjugated anti-HRP (1:250, Jackson ImmunoResearch laboratories), rabbit anti-Tkv (1:500, Dudu et al. 2006), rabbit anti-PS1 (p-Mad) (1:500; a gift from P. ten Dijke), guinea pig anti-Dnrx (1:250, Li et al., 2007), and guinea pig anti-Dnlg1 (1:250, Mozer and Sandstorm, 2012). Mouse monoclonal anti-Dlg (1:500, 4F3), anti-BRP (1:250; NC82) and anti-Wit (1:25, 23C7) were obtained from Developmental Studies Hybridoma Bank (DSHB), University of Iowa. Secondary antibodies conjugated to Alexa 488 and 568 (Invitrogen-Molecular Probes) were used at 1:200 dilution.

2.3 Immunoblotting, Immunoprecipitations and Sucrose Density Gradient Centrifugation

3rd instar larval musculature or VNC and brain lobes without any attached imaginal discs were homogenized in ice-cold RIPA buffer. The supernatants with equal amounts of proteins from each genotype were separated on SDS-PAGE for immunoblotting with respective antibodies. For immunoprecipitations (IP) studies and sucrose density gradient analysis, wild type, *dnrx/Df(3R)5C1, dnlg1*$^{\Delta 46}$, fly heads were processed according to previously described protocols (Banerjee et al., 2006). Each experiment was done independently three times and the most representative blots are shown.

Primary antibodies used for immunoblotting were anti-Dnrx (1:250), anti-Dnlg1 (1:500), anti-Wit (1:1000; DSHB), and anti-β Actin (1:10,000, 4967S, Cell Signaling).

Composition of the various buffers used are:

RIPA buffer: 150mM sodium chloride, 1% Igepal CA630, 0.5% Deoxycholate, 0.1% SDS and 50mM TrisHCl, pH 8.0.

Lysis Buffer for Immunoprecipitations: 50mM HEPES pH 7.5, 10mM NaCl, 1mM $MgCl_2$, 1mM $CaCl_2$, 0.5% Deoxycholate, 1% NP-40, 0.5% Triton X-100, and protease inhibitors.

Lysis Buffer for Sucrose Density Gradient Analysis: 10 mm Tris-HCl, pH 7.4, containing 100 mm NaCl, 10 mm EDTA, 1 mm PMSF, and 0.5% Triton X-100 and protease inhibitors.

2.4 Quantification and Statistical Analysis

Bouton number quantifications (n= number of larvae analyzed) were performed from muscles 6/7 of abdominal segment 3 (A3) by staining of the body wall muscle preparations with anti-HRP and anti-Dlg.

Image J (NIH, USA) was used for quantification of band intensities of western blots from three independent experiments. The intensity of the bands of interest was divided by their respective Actin protein to control for any possible unequal loading.

Fluorescence intensity measurements for Dnrx, Dnlg1, Dlg, Tkv and pMad were quantified from confocal slices of Z-stack images compressed using maximum projection functions, which were stained in combination with either NC82 (Fig. 1) or anti-Hrp antibodies (Figs. 3 and 8). Same regions of interest were selected for each channel and used for assessment and quantification of fluorescence intensity using Image J. At least 30 NMJ branches from 8 larvae were analyzed for various genotypes in Figs. 1, 3 and 8. All genotypes listed under the same quantification groups were stained, and processed for imaging and quantified under identical parameters and settings.

All statistical analyses were performed using the Graphpad PRISM software and data are presented as mean ± SEM. Statistical significance was determined by one way ANOVA followed by post hoc Tukey's multiple comparison test and Student's t-test. Error bars represent mean ± SEM (***$p<0.001$, **$p\leq0.01$, *$p\leq0.05$, ns – not significant).

For all quantification, the statistical significance immediately above the bars is with respect to the control genotype for that experimental group.

2.5 RNA extraction and qRTPCR Analysis

Wandering third instar larvae were collected from wild type, *dnrx, dnlg1* and *wit* mutants and washed twice and dissected in 1XPBS. Larval musculature and brain lobes/VNC were isolated, separated and transferred to RNA Later™ reagent (Sigma-Aldrich, St. Louis, MO) on ice. RNA was extracted using the QIAGEN RNAeasy kit (Thermo Fisher, Waltham, MA). cDNA was synthesized using Superscript III first strand synthesis kit (Thermo Fisher, Waltham, MA) with random oligoDT primers and used for qRTPCR analysis. qRTPCR assay was performed using the following taqman primers for the indicated genes.

Cyclophilin

F – TCTTATGGATCGCAGTCTGG

R – TTGCATCGCACCTTCTTAAA

Probe – CAAGACCTCCAAGAAGATCATTGTGGC

dnrx

F – ATTGCCGAGTAACACCAACA

R – GCTGTGTTTCTGTCGCGTAT

Probe – TCCAGTCCTTGAGCGCGAGC

dnlg1

F – AGACAACATTCGGCCCTAAC

R – AATGGGAGTGGTTCCTCAAG

Probe – CGAACCGAGTGATGAAATCCTCCA

wit

F – CTGCGGAACAGGGAATAAAT

R – TAGTGTCGGAGCTCATCTGG

Probe – ACAACGGCGGCTGCAGTCC

qRTPCR assay was performed as per manufacture's recommendation using taqman fast advanced Master mix (Thermo Fisher, Waltham, MA) on a Step one plus™ system (V2.0, Applied Biosystems). All CTs were normalized to Cyclophilin, used as a control. Levels of mRNA expression were further normalized to wild type control for individual genes. Three independent RNA extractions were performed for each genotype and qRTPCR assays were carried out in triplicates for each experiment. Statistical analysis was performed using the Graphpad Prism program.

2.6 Electron Microscopy and Morphometric Analysis

For ultrastructural analyses, third-instar larval fillets were dissected in ice-cold, Jan's 0.1mM Ca^{2+} saline, pH 7.2, and subsequently fixed in 4% paraformaldehyde/1% glutaraldehyde/0.1 M cacodylic acid, pH 7.2 for 30 minutes at room temperature followed by overnight fixation at 4°C. The fixed fillets were rinsed 3X in 0.1M cacodylic acid, pH 7.2 and postfixed in 2% aqueous osmium tetroxide for 1 hour, followed by rinsing and dehydration in increasing ethanol concentration. Samples were incubated for an hour in propylene oxide and gradually infiltrated in increasing resin to propylene oxide ratio (1:2, overnight; 2:1, at least 6 hours; and full resin for 36 hours with constant agitation). Samples were embedded in flat silicone molds with Polybed resin and cured in the oven at 55°C for 36 hours.

Three larvae were processed for EM analysis from each of the genotypes shown in Figures 4 and 7. The number of boutons (n) analyzed for each genotype is indicated in respective figures/legends. Image J was used for morphometric analysis of EM images of only Type 1b boutons from A2 and A3 as previously described (Chen et al. 2012; Li et al. 2007).

3. Results

3.1 Role of Extracellular and Intracellular Regions of Dnrx and Dnlg1 in Synaptic Clustering of Dnlg1 and Dnrx

Previous studies have shown that presynaptic *dnrx* and postsynaptic *dnlg1* mutants show about 50% reduction in synaptic boutons at their respective mutant NMJs besides displaying other similarities in morphometric parameters compared to their wild type counterparts (S. Fig. 1) (Li et al., 2007; Banovic et al., 2010; Mozer and Sandstrom, 2012). Bouton numbers at the larval NMJ in *dnlg1, dnrx* double mutants are similar to *dnlg1* and *dnrx* single mutants (S. Fig. 1; Banovic et al., 2010) suggesting that Dnrx and Dngl1 function together to regulate synaptic growth. We wanted to analyze the synaptic clustering of endogenous Dnlg1 and Dnrx in each other's mutant backgrounds to determine if they were altered (Fig. 1). Wild type (+/+) Dnlg1 localizes to the postsynaptic terminal of the synaptic boutons (Fig. 1Aa,c) surrounding, but not overlapping, with the active zones labeled by anti-Bruchpilot (NC82) (Fig. 1Ab,c). While, as expected, Dnlg1 is absent in *dnlg1* mutants (Fig. 1Ca,c), it fails to localize properly and shows sparse clustering in the synaptic boutons of *dnrx* mutants (Fig. 1Ba,c) surrounding the active zones (Fig. 1Bb,c). Dnlg1 also shows a significant reduction in levels in *dnrx* mutant boutons consistent with previously published observations (Fig. 1B; quantified in Fig. 1M; Banovic et al. 2010). These immunofluorescence observations were further corroborated by western blot analysis where lysates from larval body wall musculature of wild type (+/+), *dnlg1* and *dnrx* mutants when probed with anti-Dnlg1 showed a significant reduction in levels of Dnlg1 protein in *dnrx* mutants compared to wild type (Fig. 1O, quantified in Fig. 1P).

Next we wanted to test whether endogenous Dnrx localization was affected in *dnlg1* mutants. Since endogenous Dnrx levels are undetectable by standard immunohistochemistry, we amplified the fluorescence signal as previously described (Li et al. 2007). Consistent with previously published reports Dnrx localization is dense in the presynaptic terminals of wild type boutons (Fig. 1Ga,c; Li et al. 2007). Dnrx is absent in *dnrx* mutants, as expected

(Fig. 1Ha,c) and shows a reduced and punctate localization in *dnlg1* mutant boutons (Fig. 1Ia,c; quantified in Fig. 1N). Our endogenous Dnrx localization data are consistent with previous reports where a decrease in levels of over-expressed Dnrx was reported when a full length Dnrx was driven presynaptically in *dnlg1* mutant background (Banovic et al. 2010). In order to check endogenous levels of Dnrx in wild type, *dnrx* and *dnlg1* mutants, we performed western blot analysis from lysates obtained from larval body wall musculature but could not detect Dnrx (data not shown) presumably due to very low levels that were beyond detection using standard immunoblot protocols. However, since Dnrx is abundantly expressed in the brain lobes and ventral nerve cord (VNC) of third instar larva (S. Fig. 2), we did western blot analysis to check if Dnrx levels are altered in *dnlg1* mutants. The quantification of band intensity ratio of both Dnlg1 (Fig. 1P) and Dnrx (Fig. 1R) with respect to Actin showed a significant reduction in their levels in each other's mutant backgrounds. Taken together, the endogenous localization studies together with immunoblot analysis of Dnlg1 and Dnrx show an interdependence of these proteins for their proper localization.

Given this interdependency between Dnrx and Dnlg1 for their localization, we were interested to see if Dnlg1 can cluster properly at the synapses if full length and truncated forms of Dnrx protein were expressed presynaptically using the presynaptic *elav-Gal4* in the *dnrx* mutant background. Dnlg1 localization was found to be significantly rescued in *elav-Gal4/UAS-dnrx;dnrx*$^{-/-}$ (Fig. 1Da,c; M) compared to *dnrx* mutants (Fig. 1Ba,c; M) but did not reach wild type levels (Fig. 1M). However, the N-terminal deletion of Dnrx when expressed presynaptically in *dnrx* mutant backgrounds could not restore proper Dnlg1 localization to the postsynaptic terminals as seen in *elav-Gal4/UAS-dnrx*$^{\Delta N}$*;dnrx*$^{-/-}$ (Fig. 1Ea,c, M). The C-terminal deletion of Dnrx as seen in *elav-Gal4/UAS-dnrx*$^{\Delta C}$*;dnrx*$^{-/-}$, on the other hand, was able to significantly restore Dnlg1 localization compared to *dnrx* mutants (Fig. 1Fa,c, M). We then wanted to investigate if Dnrx presynaptic clustering could be restored in *dnlg1* mutants when full length and truncated forms of Dnlg1 were expressed using the muscle driver, *mef2-Gal4* (Fig. 1J). Dnrx was able to localize properly in the full length rescue seen in *mef2-Gal4/UAS-dnlg1;dnlg1*$^{-/-}$ (Fig. 1Ja,c, quantified in Fig. 1N), which was not only a significant improvement when compared to the *dnlg1* mutants alone (Fig. 1Ia,c) but the rescue level reached close to wild type (Fig. 1N). However, Dnrx was not recruited to the presynaptic terminals either when a N-terminal deletion of Dnlg1 was expressed postsynaptically as seen in *mef2-Gal4/UAS-dnlg1*$^{\Delta N}$*;dnlg1*$^{-/-}$ (Fig. 1Ka,c, N), or in a C-terminal deletion of Dnlg1 as seen in *mef2-Gal4/UAS-dnlg1*$^{\Delta C}$*;dnlg1*$^{-/-}$ (Fig. 1La,c, N). These data indicate that both the extracellular and cytoplasmic regions of Dnrx and Dnlg1 are necessary for proper synaptic clustering of Dnlg1 and Dnrx, respectively.

3.2 Neurexin and Neuroligin 1 Exist as a Biochemical Complex

Since *dnrx* and *dnlg1* function in a common pathway regulating synaptic growth (S. Fig. 1) and also show interdependence for proper localization to the synaptic terminals, we performed extensive biochemical analyses to study whether the trans-synaptic complex of Dnrx and Dnlg1 are part of a macromolecular protein complex in the nervous system and what biochemical properties this trans-synaptic complex might have. For these biochemical studies, besides the immunoblot analysis described in the preceding section 3.1 (Fig. 1O-R),

we examined: 1) whether Dnrx and Dnlg1 associate in a biochemical complex by coimmunoprecipitation (IP) assays, and 2) how Dnrx and Dnlg1 distribute in a sucrose buoyant density gradient separation.

Since Dnrx and Dnlg1 are not abundant in the same larval tissue types, with Dnrx being more abundant in the brain lobes/VNC (Fig. 1Q; S. Fig. 2) where Dnlg1 is undetectable and Dnlg1 being highly expressed in larval musculature (Fig. 1O; S. Fig.2) where Dnrx is undetectable (data not shown), we decided to utilize the adult *Drosophila* heads for the remainder of our biochemical analysis where both Dnrx and Dnlg1 were present at detectable levels. We first performed co-IP experiments to examine if Dnrx and Dnlg1 associate in a biochemical complex. Immunoblots on wild type (+/+) head lysates showed presence of Dnlg1 (Fig. 1S) and Dnrx (Fig. 1T) both of which are absent in their respective mutant lysates. IP experiments using Dnlg1 and Dnrx efficiently precipitated Dnlg1 (Fig. 1Ua) and Dnrx (Fig. 1V), respectively. The specificity of the IPs was confirmed from the absence of Dnlg1 (Fig. 1Ua) and Dnrx (Fig. 1V) in *dnlg1* and *dnrx/Df(3R)5C1* (genotypic combination to obtain viable adults) mutant head lysates, respectively. Co-IP experiments using Dnlg1 could detect presence of Dnrx (Fig. 1Ub) suggesting that Dnlg1 and Dnrx exist as a protein complex.

In addition, we performed sucrose density gradient analysis of fly head lysates from wild type, *dnlg1* and *dnrx/Df(3R)5C1* to determine: i) how Dnlg1 and Dnrx distribute in a buoyant gradient, ii) whether they distribute in overlapping fractions and finally, iii) whether the distribution of each protein is altered in the mutant background of the other. As shown in Fig. 1Wa and Xa, Dnrx and Dnlg1 co-sediment in overlapping fractions (lanes 7–15) indicating that these proteins are associated with subcellular structures of same density and may associate in biochemical complex that is partially maintained during subcellular fractionation. Interestingly, Dnrx (Fig. 1Wa) and Dnlg1 (Fig. 1Xa) distributions are in identical fractions (lanes 7–15) in the wild type (+/+) gradient suggesting a strong association between the two proteins. It is important to note that distributions of Dnrx (Fig. 1Wb) shifts to the lighter fractions in *dnlg1* mutants. Similarly, Dnlg1 (Fig. 1Xc) is detected in the lighter sucrose density fractions in *dnrx* mutants. As is evident Dnrx and Dnlg1 levels are significantly reduced in the mutant backgrounds of *dnlg1* and *dnrx* mutants, respectively, compared to wild type (compare Fig. 1Wb with 1Wa; and 1Xc with 1Xa) indicating reduced stability similar to what was observed in the larval nervous system. Taken together, the biochemical analysis reveals an in vivo molecular association between Dnrx and Dnlg1 suggesting that these proteins exist in a large macromolecular complex.

3.3 Domain-Specific Requirements of Dnrx and Dnlg1 in Synaptic Growth

The localization studies of Dnrx and Dnlg1 using domain-specific truncations of these two proteins in each other's mutant backgrounds pointed towards a requirement of both the extracellular and cytoplasmic domains for their proper localizations. We wanted to take advantage of the domain-specific truncations of Dnlg1 and Dnrx and extend our studies to look at which domains of these proteins are required for proper synaptic growth. As previously reported, overexpression of Dnrx in the wild type background in all neurons showed excessive growth of synaptic boutons (Fig. 2C, I; Li et al. 2007) compared to wild

type controls (+/+, Fig. 2A, I). Further, it was observed that the synaptic undergrowth phenotype of *dnrx* mutants (Fig. 2B, I) was significantly rescued upon presynaptic expression of full length Dnrx (Fig. 2D, I). We next wanted to determine the consequences of overexpression of Dnrx lacking either the extracellular (Fig. 2E) or the cytoplasmic regions (Fig. 2G) in a wild type background on synaptic growth using the *elav-Gal4* driver. Larval NMJs of *elav-Gal4/UAS-dnrx*$^{\Delta N}$ (Fig. 2E, I) and *elav-Gal4/UAS-dnrx*$^{\Delta C}$ (Fig. 2G, I) showed no significant changes in the total number of synaptic boutons compared to the wild type controls (Fig. 2A, I) suggesting that the truncated proteins do not cause any dominant negative effects by interfering with the endogenous protein function. Next we wanted to study the effects of overexpressing the truncated Dnrx proteins presynaptically in the *dnrx* mutant background in an attempt to rescue the synaptic growth. The deletion of extracellular domain of Dnrx in *elav-Gal4/UAS-dnrx*$^{\Delta N}$*;dnrx*$^{-/-}$ presented a severe reduction in the number of synaptic boutons (Fig. 2F, I) compared to wild type (Fig. 2A, I). The bouton numbers in *elav-Gal4/UAS-dnrx*$^{\Delta N}$*;dnrx*$^{-/-}$ (Fig. 2F, I) showed no significant difference compared to the *dnrx* mutants (Fig. 2B, I). While the cytoplasmic domain truncation of Dnrx in *elav-Gal4/UAS-dnrx*$^{\Delta C}$*;dnrx*$^{-/-}$ had a significant increase in the synaptic bouton numbers (Fig. 2H, I) compared to the *dnrx* single mutants (Fig. 2B, I), the synaptic growth was restored to wild type levels (Fig. 2I). These data suggest that the extracellular domain of Dnrx is critical for its synaptic growth function. On the other hand, both the extracellular and cytoplasmic regions of Dnlg1 were required for proper synaptic growth, as has been reported previously (S. Fig. 3; Banovic et al. 2010). Together, the deletion analyses highlight the importance of the extracellular domain of Dnrx, and both the extra- and intracellular regions of Dnlg1 in proper synaptic growth at NMJ.

3.4 Loss of Dnrx and Dnlg1 Affects Subcellular Localization of Discs large, a Subsynaptic Reticulum Protein

Apart from the localization and synaptic growth studies using single and double mutants of *dnrx* and *dnlg1*, as well as the domain truncated forms of Dnrx/Dnlg1, we were interested in studying if these mutants caused any aberrations in the organization or differentiation of postsynaptic specializations. To this end, we looked at the subcellular localization of Discs large (Dlg), a key protein that assembles the subsynaptic reticulum (SSR) in Type 1b boutons (Lahey et al. 1994; Budnik et al. 1996). Dlg localizes to an intricate system of highly convoluted membrane, called the SSR that surrounds the postsynaptic muscle of the Type 1b boutons. Confocal microscopy of Dlg immunoreactivity (Fig. 3, red) together with the neuronal membrane marker, HRP (Fig. 3, green) in wild type (+/+) revealed a strong localization in the peripheral borders of Type 1b boutons and in a perisynaptic network, and is excluded from the core of the boutons (Fig. 3Aa,b; Lahey et al. 1994). Dlg localization in *dnrx* mutants, although still at the SSR, is significantly lower in intensity (Fig. 3Ba,b, G) compared to wild type (+/+, Fig. 3Aa, G). Interestingly, while a vast majority of *dnlg1* mutant boutons display mislocalization of DLG in the form of a more uniform distribution throughout the entire bouton as opposed to a more specific localization seen in the wild type SSR (compare Fig. 3Aa with Fig. 3Ca), the fluorescence intensity ratio of Dlg/Hrp in *dnlg1* mutants stayed unchanged compared to wild type (Fig. 3G). Upon quantification of Dlg localization that is enriched at the SSR versus a more uniform diffuse localization throughout the bouton in *dnlg1* mutants, we found <10% boutons with some enrichment of

Dlg in SSR and >90% boutons with a uniform distribution of Dlg compared to wild type boutons that show near 100% enrichment of Dlg in SSR. Double mutants of *dnlg1,dnrx* displayed a combination of their respective single mutant phenotypes with a reduction in Dlg intensity (Fig. 3Da,b, G) as well as a misdistribution and failure to localize to the SSR (Fig. 3Da,b). Postsynaptic expression of full length Dnlg1 in the mutant *dnlg1* background as seen in *mef2-Gal4/UAS-dnlg1;dnlg1*$^{-/-}$ (Fig. 3Ea,b) rescued the subcellular localization of Dlg. These data suggest that the Dnlg1 is important for proper Dlg localization and recruitment to the SSR of type 1b boutons. It is important to note that there was no significant difference in ratio of immunofluorescence intensities of Dlg/HRP at the synaptic boutons in wild type, *dnlg1* mutants and it's rescue (Fig. 3H) suggesting that it is the proper localization of Dlg that is affected and not the levels of the Dlg protein.

Similar rescue studies were performed in *dnrx* mutants to examine whether full length Dnrx protein when expressed presynaptically could restore the subcellular localization and/or levels of Dlg. Indeed full length Dnrx when expressed in the mutant *dnrx* backgrounds as seen in *elav-Gal4; UAS-dnrx;dnrx*$^{-/-}$ (Fig. 3Fa,b, I) restored the subcellular localization and levels of Dlg similar to the wild type controls (Fig. 3Aa, I). Taken together these studies indicate that loss of presynaptic Dnrx and/or postsynaptic Dnlg1 lead to a clear alteration in the pattern of subcellular Dlg localization, suggestive of a possible alteration in the postsynaptic differentiation and SSR ultrastructure in the single and double mutants of *dnlg1* and *dnrx*.

3.5 Pre- and Post-Synaptic Ultrastructural Abnormalities in *dnrx* and *dnlg1* Single and Double Mutants

The altered subcellular localization of Dlg seen in the single and double mutants of *dnrx* and *dnlg1* led us to analyze the ultrastructure of the synaptic boutons in these mutants. The initial characterization of synaptic ultrastructural deficits of *dnrx* and *dnlg1* single mutants, although reported separately, showed commonalities in certain phenotypes (Li et al. 2007; Banovic et al. 2010). However, since there are no existing studies on the combined loss of *dnrx* and *dnlg1*, we wanted to investigate the consequences of simultaneous loss of these two key trans-synaptic adhesion proteins in the organization of the overall synaptic architecture and how that compared with individual mutants and wild type controls.

For ultrastructural studies, the wild type and mutant boutons were serially sectioned and analyzed. The wild type boutons are characterized by distinct pre- and postsynaptic membrane that is closely apposed to each other (Fig. 1A, J). The presynaptic compartment contains synaptic vesicles, apart from organelles such as mitochondria. The presynaptic membrane has active zones composed of electron dense structures called T-bars (Fig. 1A, F; Wagh et al. 2006). At the postsynaptic muscle, the type 1b boutons are surrounded by the SSR. Some of the key ultrastructural defects reported earlier for both *dnrx* and *dnlg1* mutants were a detachment of the presynaptic membrane from the postsynaptic side leading to a ruffling membrane morphology and reduced SSR thickness compared to the wild type (Li et al. 2007; Banovic et al. 2010). We performed serial sectioning of boutons from wild type, single and double mutants of *dnrx and dnlg1* and subjected them to morphometric

analyses to determine which of these phenotypes increased in severity, if at all, upon the loss of each or both of these proteins.

Our analysis did not show any significant increase in the overall area of the boutons in single and double mutants of *dnrx* and *dnlg1* (Fig. 4B, C, D, N) compared to wild type (Fig. 4A, N). However, in *dnrx,dnlg1* double mutants we observed some giant boutons that were laterally elongated with multiple active zones and reduced SSR (Fig. 4E). The number of active zones (asterisks, Fig. 4B-D, O), total PSD length (Fig. 4B-D, P) and presynaptic membrane ruffles (Fig. 4G-I, Q, arrowheads) showed a significant increase in the single and double mutants of *dnrx* and *dnlg1* when compared to the wild type (Fig. 4O-Q). However, these phenotypes were not significantly different when single mutants of *dnrx* and *dnlg1* and the double mutants were compared against one another (Fig. 4O-Q). The postsynaptic phenotypes, such as the normalized SSR width (Fig. 4R), the SSR density (number of membrane folds/μM) (Fig. 4S) showed a significant reduction in the both single and double mutants of *dnrx* and *dnlg1* when compared to wild type (Fig. 4A, R, S). It is interesting to note that while the SSR density (Fig. 4S) did not show any significant difference between the single and double mutants, the normalized SSR width showed a significant reduction in *dnrx, dnlg1* double mutants (Fig. 4D, R) compared to the single mutants alone (Fig. 4B, C, R). Another phenotype that was prominent in a subset of *dnrx,dnlg1* double mutant boutons was the presence of large membranous folds in the presynaptic terminals (data not shown) which could be reflective of a problem with the underlying cytoskeleton (Ashley et al. 2005). The overall SSR morphology in mutants was less extensive and less complex showing reduced folding of the subsynaptic membranes (Fig. 4K-M) compared to wild type control (+/+, Fig. 4J). Taken together these data show that loss of Dnrx and Dnlg1 leads to defective ultrastructural organization of both the pre- and postsynaptic areas at the NMJ.

3.6 Loss of Dnrx and Dnlg1 Affects the Localization and Stability of the Presynaptic Receptor, Wishful Thinking

To identify other synaptic mutants that phenocopied *dnrx* or *dnlg1* mutants, we pursued *wit* mutants as they display stunted growth of NMJ synapses, and detachments of presynaptic membrane (Aberle et al., 2002; Marques et al., 2002). Phenotypic similarities between *dnrx, dnlg1* and *wit* suggested the possibility of these three trans-synaptic players functioning in common developmental programs that impact synaptic growth and overall synaptic architecture. These observations also led us to hypothesize that Dnrx, Dnlg1 and Wit might be interdependent for their proper localization and/or stability and may work in coordination at the NMJ.

We first wanted to look at the endogenous Wit levels (using anti-Wit, 23C7, DSHB) in larvae of wild type, *dnlg1, dnrx* and *wit* mutants by immunoblot analyses. Equal amounts of protein lysates from larval musculature (Fig. 5A) of wild type (+/+), *dnlg1, dnrx* and *wit* showed a complete loss of Wit in $wit^{A12/B11}$ mutants, and a significant reduction of Wit in *dnlg1* and *dnrx* mutants (Fig. 5A, B) using anti-Actin as loading control (Fig. 5A, B). We further wanted to know if the severe reduction in Wit protein levels was due to reduced stability or less mRNA levels. qRTPCR analysis using *wit* mRNA from wild type, *wit, dnlg1* and *dnrx* mutants did not reveal any significant differences in mRNA levels between these

genotypes indicating that the reduction in Wit levels was due to reduced stability of Wit in *dnrx* and *dnlg1* mutants (Fig. 5C). Next, we performed sucrose density gradient analysis of fly head lysates from wild type, *dnlg1* and *dnrx/Df(3R)5C1* to determine how Wit distributes in a buoyant density gradient with respect to Dnlg1 and Dnrx, and whether Wit distribution is affected in *dnrx* and *dnlg1* mutants. Since $wit^{A12/B11}$ flies fail to eclose as adults, we could not determine whether loss of Wit reciprocally affected the distribution of Dnlg1/Dnrx in *wit* mutant head lysates. Although Wit is detected in lighter gradient fractions (as seen in fraction 4; Fig. 5Da), it is enriched in fractions 7–11 overlapping with both Dnrx (compare Fig. 5Da with Fig. 1Wa) and Dnlg1 (compare Fig. 5Da with Fig. 1Xa) indicating that these proteins are associated in a biochemical complex that is partially maintained during subcellular fractionation. It is important to note that distributions of Wit shifts to the lighter fractions in *dnlg1* mutants (Fig. 3Db). Consistent with the endogenous levels of Wit in the *dnrx* and *dnlg1* larvae, Wit levels is significantly reduced in the mutant backgrounds of either *dnrx* or *dnlg1* head lysates when compared to wild type protein levels (compare Fig. 5Db, c with Fig. 5Da) indicating a reduced stability similar to what was observed in the larval nervous system. Taken together, the biochemical analyses reveal an in vivo molecular association between Dnrx, Dnlg1 and Wit suggesting that these proteins exist in a large macromolecular protein complex.

The reduction in Wit levels in *dnrx* and *dnlg1* mutants prompted us to determine whether the endogenous localization of Dnrx and/or Dnlg1 was affected in *wit* mutants. Dnrx localization in *wit* mutant NMJ (Fig. 5Fa,c) was decreased considerably and displayed a punctate pattern (compared to the dense localization in the corresponding wild type terminals shown in Fig. 5Ea,c), while Dnlg1 in *wit* mutants showed no major changes (Fig. 3Ha, c) compared to wild type (Fig. 3Ga,c). We next attempted to study the immunolocalization of endogenous Wit in wild type, *dnrx, dnlg1* and *wit* (wit^{A12}/wit^{B11}) mutant NMJs, but despite our best efforts, the endogenous Wit levels were undetectable with standard immunohistochemistry protocols using anti-Wit antibodies. We also tried to artificially enhance Wit signal at NMJ to aid in its detection as done previously for Dnrx but were unable to detect endogenous Wit. The inability to detect endogenous Wit has been reported previously (Nahm et al. 2013). To circumvent this limitation, we adopted the same strategy as Nahm et al. 2013 where *UAS-wit* was overexpressed presynaptically using the *elav-Gal4* driver (Fig. 5I-L). By this method we could detect Wit immunoreactivity at the synaptic boutons of *elav-Gal4;UAS-wit* larvae (Fig. 5Ib,c, Kb,c; Nahm et al., 2013). Next we wanted to determine whether Wit was affected in *dnrx* and *dnlg1* mutants by generating *elav-Gal4;UASwit;dnrx*$^{-/-}$ (Fig. 5J) and *elav-Gal4;UAS-wit;dnlg1*$^{-/-}$ (Fig. 5L), respectively, and compared the Wit levels with *elav-Gal4;UAS-wit* larvae as control (Fig. 5Ib,c and 5Kb,c). Upon immunostaining with anti-Wit, we detected significantly reduced levels of Wit at the NMJ in both *dnrx* and *dnlg1* mutant backgrounds (Fig. 5Jb,c and Lb,c, respectively) suggesting that Wit requires Dnrx and Dnlg1 for its proper clustering at the NMJ. Together these data demonstrate that Dnrx and Dnlg1 are required for both the localization and stability of Wit at the NMJ.

3.7 *dnrx* and *dnlg1* Display Genetic Interactions with *wit*

Given the interdependency of protein localization (Fig. 5) and a common synaptic undergrowth phenotype seen in *dnrx, dnlg1* and *wit* mutants (Aberle et al., 2002; Marques et al., 2002; Li et al. 2007, Banovic et al. 2010; Mozer et al. 2012), we wanted to examine if *wit,dnrx* and *wit,dnlg1* displayed genetic interactions with respect to NMJ phenotypes. We analyzed the total bouton numbers in *wit/+* and found no difference compared to the wild type (Fig. 6A, L). We next analyzed bouton numbers in double heterozygous combinations of *wit/+,dnrx/+* (Fig. 6C, L) and *wit/+,dnlg1/+* (Fig. 6D, L) and found a significant reduction compared to the single heterozygotes (*wit/+, dnrx/+* and *dnlg1/+*, Fig. 6L) and wild type (Fig. 6L) indicating that these genes may function together in regulating synaptic growth. Comparison of bouton counts in single mutants of *wit, dnrx* and *dnlg1* did not show any significant differences between one another (Fig. 6M). Double mutants of *wit−/−, dnrx−/−* (Fig. 6E, M) and *wit−/−,dnlg1−/−* (Fig. 6F, M) had bouton numbers that were not significantly different than *wit−/−* single mutants (Fig. 6B, M). Double mutants of *wit−/−,dnrx−/−* (Fig. 6E, M) and *wit−/−,dnlg1−/−* (Fig. 6F, M), on the other hand, displayed a considerable severity in the reduction of synaptic boutons when compared to *dnrx* and *dnlg1* single mutants, respectively (Fig. 6M). These data indicate that *wit,dnrx* and *wit,dnlg1* display genetic interactions, and are involved in coordinating synaptic growth at NMJ.

Our next set of studies were designed to test whether removal of one copy of *wit* as seen in *elav-Gal4; UAS-dnrx; wit/+* (Fig. 6H) could attenuate the synaptic overgrowth phenotype that resulted from the presynaptic overexpression of Dnrx (*elav-Gal4; UAS-dnrx;* Fig. 6G). Quantification of bouton numbers from *elav-Gal4; UAS-dnrx* (Fig. 6G, N) and *elav-Gal4; UAS-dnrx; wit/+* (Fig. 6H, N) did not show any significant difference. We next examined whether synaptic overgrowth phenotype resulting from the presynaptic overexpression of Dnrx required Wit function. Immunostaining of *elav-Gal4; UAS-dnrx; wit−/−* (Fig. 6I, N) did not show any increase in bouton numbers when compared to *wit−/−* (Fig. 6B) indicating that Wit is required for Dnrx-mediated synaptic growth. Finally, we wanted to determine the consequences of presynaptic Wit overexpression in *dnrx* mutant background. Wild type Wit overexpression as seen in *elav-Gal4; UAS-wit* (Fig. 6J, N) did not exhibit any significant difference in bouton numbers compared to the wild type controls (Fig. 6N). Wit, when overexpressed presynaptically in *elav-Gal4; UAS-wit; dnrx−/−* larvae (Fig. 6K, N), had bouton numbers similar to *dnrx−/−* single mutants alone suggesting that Wit overexpression cannot rescue the reduced synaptic growth of *dnrx* mutant. These data provide strong support that trans-synaptic adhesive mechanisms involving Dnrx and Dnlg1 must work in close coordination with the synaptic signaling mechanisms mediated by Wit to allow proper synaptic growth at NMJ.

3.8 Combined Loss of Wit with Dnrx or Dnlg1 Leads to Synaptic Organization Defects

The genetic interaction studies of *dnx, dnlg1* and *wit*, together with the dramatic reduction in Wit stability seen from loss of Dnrx and Dnlg1 led us to postulate that there might be adhesive interactions between these three proteins across the synaptic apparatus that gets disrupted in the event of a loss of one or more combination of these proteins. To address this, we conducted ultrastructural analysis of the synaptic boutons of *wit* single and *wit,dnrx* and *wit,dnlg1* double mutants. The initial published reports on synaptic ultrastructure of *wit*

single mutants revealed a similar ruffling morphology caused by the detachment of the presynaptic membrane also seen in *dnrx* and *dnlg1* single mutants (Aberle et al. 2002; Marques et al. 2002; Li et al. 2007; Banovic et al. 2010; this study). The generation of the double mutants of *wit,dnrx* and *wit,dnlg1* for our genetic interaction studies also provided us with an opportunity to study the ultrastructural deficits that are presented when two key presynaptic transmembrane proteins, Wit and Dnrx are lost as well when a trans-synaptic combination of Wit and Dnlg1 are absent.

Serial sectioning of boutons from wild type (Fig. 7A), *wit* single mutants (Fig. 7B), *wit,dnrx* (Fig. 7C) and *wit,dnlg1* (Fig. 7D) double mutants were subjected to morphometric analyses. While *wit* single mutants, *wit,dnrx* and *wit,dnlg1* double mutants had similar bouton area compared to wild type (Fig. 7M), *wit* single mutants had a modest but significant increase in bouton area than *wit,dnlg1* double mutants (Fig. 7M). The number of active zones (asterisks, Fig. 7A-D, N), total PSD length (Fig. 7A-D, O) and presynaptic membrane ruffles (Fig. 7J-L, P, arrowheads) showed a significant increase in *wit* single mutants, *wit,dnrx* and *wit,dnlg1* double mutants when compared to the wild type (Fig. 7A, I, N-P). However, there were no changes in these phenotypic parameters among the mutants (Fig. 7M-P). Interestingly, loss of presynaptic *wit* alone as well as combined loss of presynaptic *wit* and *dnrx* displayed postsynaptic phenotypes that were similar to double mutants of *wit,dnlg1*. Postsynaptic SSR morphology was severely compromised in both the single and double mutants (arrow, Fig. 7 B-D, higher magnification shown in F-H) compared to wild type (Fig. 7A, E). Quantification of SSR width (Fig. 7Q) and SSR density (Fig. 7R) showed a highly significant reduction in the single and double mutants compared to wild type. Interestingly, the SSR width (Fig. 7Q) and the SSR density (Fig. 7R) were indistinguishable among the mutants and showed no statistical significance. The overall SSR morphology in mutants was less extensive with thinner folds of the subsynaptic membranes (Fig. 7B-D and F-H). It is, however, worth mentioning that the double mutants display some phenotypes that were not typically encountered in *wit* single mutant or wild type. One such phenotype was the presence of large synaptic vesicles in the presynaptic region in both double mutants (asterisks, Fig. 7K, L), which could be indicative of synaptic disassembly and degeneration or a nerve terminal retraction (Eaton et al. 2002; Pielage et al. 2005). Taken together these studies provide evidence that Wit, Dnrx and Dnlg1 function in close coordination to allow proper assembly and organization of the overall synaptic architecture, which is critical for NMJ growth and function.

3.9 Loss of Dnrx and Dnlg1 Affect Levels of pMad and Tkv at NMJ

Apart from the Type II BMP receptor Wit, we wanted to further investigate whether Dnrx and Dnlg1 regulate the levels of Type I receptor(s) and/or downstream effector of the BMP pathway at the NMJ synapses. To that end, we first tested the levels of the Type I BMP receptor, Tkv. Consistent with previous reports, Tkv localizes in the synaptic boutons including the SSR surrounding the presynaptic terminals labeled by HRP (Fig. 8Aa,b; Dudu et al. 2006). Low levels of Tkv are also detected in presynaptic boutons (Fig. 8Aa; Dudu et al. 2006). Compared to wild type controls, we observed a significantly reduced level of Tkv in *dnrx* and *dnlg1* mutant synaptic boutons (compare Fig. 8Ba,b and Ca,b with Aa,b;

quantified in Fig. 8O), while no difference was observed in the levels of Tkv in *wit* mutants (compare Fig. 8Da,b with Fig. 8Aa,b; O).

Since levels of both Type II BMP receptor Wit and Type I receptor Tkv are reduced in *dnrx* and *dnlg1* mutants, we hypothesized that this will cause a reduction in the phosphorylation of the R-Smad, Mad at the NMJ terminals. Mad is a downstream effector of the BMP signaling pathway at the NMJ and receptor activation upon ligand binding leads to an increase in Mad phosphorylation (pMad) (Merino et al. 2009). pMad labeled by anti-PS1 show a distinct localization as puncta decorating the synaptic boutons in control wild type larvae (Fig. 8Ea). Synaptic boutons co-labeled with anti-pMad and anti-HRP show a marked decrease in pMad intensity in both *dnrx* and *dnlg1* mutant boutons compared to wild type (compare Fig. 8Fa,b and Ga,b with Ea,b; quantified in Fig. 8P). *wit* mutants showed an even more diminished level of pMad at the NMJ boutons (Fig. 8Ha,b; quantified in Fig. 8P; Sulkowski et al. 2014) compared to wild type, *dnrx* and *dnlg1* mutants. Taken together, these data demonstrate that Dnrx and Dnlg1 regulate receptor levels as well as downstream effectors of the BMP pathway.

We next wanted to examine whether *dnrx* and *dnlg1* show any genetic interactions with one of the downstream components of *wit*. We chose to test if *Mad;dnrx* and *Mad;dnlg1* displayed genetic interactions with respect to synaptic growth at the NMJ. We analyzed the total bouton numbers in *Mad/+ larvae* and found no difference when compared to the wild type (Fig. 8I, Q). We next analyzed bouton counts in double heterozygous combinations of *Mad/+;dnrx/+* (Fig. 8J, Q) and *Mad/+;dnlg1/+* (Fig. 8K, Q) and found a significant reduction compared to the single heterozygotes (*Mad/+*, Fig. 8Q; *dnrx/+* and *dnlg1/+*, data not shown) and wild type (Fig. 8Q) indicating that a combined reduction of gene dosage severely affects synaptic growth. Comparison of bouton counts in single mutants of *Mad, dnrx* and *dnlg1* did not show any significant differences between one another. Double mutants of *Mad−/−*; *dnrx −/−* (Fig. 8M, Q) and *Mad−/−;dnlg1−/−* (Fig. 8N, Q) had bouton numbers that were not significantly different than *Mad* (Fig. 8L, Q), *dnrx* and *dnlg1* single mutants (S. Fig. 4). Together, these data indicate that *Mad* genetically interacts with *dnrx* and *dnlg1* and that Dnrx, Dnlg1 trans-synaptic complex is coordinately linked with the BMP signaling pathway to synchronize pre- and post-synaptic adhesion with bouton growth at NMJ synapses.

4. DISCUSSION

Neurexins and Neuroligins have emerged as major players in the organization of excitatory and inhibitory synapses across species. Mutational analyses in *Drosophila* uncovered specific functions of Dnrx and Dnlg1 in NMJ synapse organization and growth, where Dnrx is expressed pre-synaptically and Dnlg1 post-synaptically. Deletion of the extracellular and intracellular regions of Dnrx or Dnlg1 revealed that both regions are necessary for Dnrx and Dnlg1 clustering and function at the synapse. Most importantly, the data presented here suggest that *dnrx* and *dnlg1* genetically interact with *wit* as well as the downstream effector of BMP signaling, *Mad* to allow both the organization and growth of NMJ synapses. The surprising finding that loss of Dnrx and Dnlg1 leads to decreased Wit stability and that Dnrx and Dnlg1 are required for proper Wit localization raises the possibility that these proteins function to coordinate trans-synaptic adhesion and synaptic growth. This is further

strengthened from the observations that, in the absence of Wit, the synaptogenic activity from overexpression of Dnrx did not manifest into an increased synaptic growth as is seen in the presence of Wit (Fig. 2; Fig. 6; S. Table 1; Li et al., 2007). Loss of Dnrx and Dnlg1 also led to a reduction in the levels of other components of the BMP pathway, namely the Tkv and pMad. Together our findings are the first to demonstrate a functional coordination between trans-synaptic adhesion proteins Dnrx and Dnlg1 with Wit receptor and BMP pathway members to allow precise synaptic organization and growth at NMJ. It would be of immense interest to investigate whether similar mechanisms might be operating in vertebrate systems.

4.1 Structure-Function Analysis of Dnrx and Dnlg1 and Synaptic Protein Clustering

The trans-synaptic cell adhesion complex formed by heterophilic binding of pre-synaptic Neurexins (Nrxs) and post-synaptic Neuroligins (Nlgs) (Ichtchenko et al., 1995) displayed synaptogenic function in cell culture experiments (Song et al., 1999; Scheiffele et al., 2000). n vertebrates and invertebrates alike, Nrxs and Nlgs belong to one of the most extensively studied synaptic adhesion molecules with a specific role in synapse organization and function (Südhof, 2008; Li et al., 2007; Banovic et al., 2010; Mozer and Sandstrom, 2012). In *Drosophila, dnrx* and *dnlg1* mutations cause reductions in bouton number, perturbation in active zone organization and severe reduction in synaptic transmission (Li et al., 2007; Banovic et al., 2010). These phenotypes are essentially phenocopied in both *dnrx* and *dnlg1* mutants, and double mutants do not cause any significant enhancement in the single mutant phenotypes illustrating that they likely function in the same pathway. From our immunohistochemical and biochemical analyses, it is evident that lack of Dnrx or Dnlg1 causes their diffuse locali ation and protein instability in each other's mutant backgrounds (Fig. 1). These data suggest that trans-synaptic interaction between Dnrx and Dnlg1 is required for their proper localization and stability, and that these proteins have a broader function in the context of general synaptic machinery involving Nrx-Nlg across phyla. It also raises the possibility that the trans-synaptic molecular complex involving Nrx-Nlg may alter stability of other synaptic proteins and lead to impairments in synaptic function without completely abolishing synaptic structure and neurotransmission (Missler et al., 2003; Varoqueaux et al., 2006; Chubykin et al., 2007; Wittenmayer et al., 2009). t is therefore not surprising that Nrx and Nlg have been recently reported to be associated with many nonlethal cognitive and neurological disorders, such as schizophrenia, ASD, and learning disability (Südhof, 2008; Banerjee et al. 2014).

The rescue studies of Dnrx and Dnlg1 localization using their respective N- and C-terminal domain truncations emphasize a requirement of the full-length protein for proper synaptic clustering (Fig. 1). Given that Dnrx and Dnlg1 likely interact via their extracellular domains, it is somewhat expected that an N-terminal deletion as seen in genotypic combinations of *elav-Gal4/UAS-Dnrx$^{\Delta N}$;dnrx−/−* and *mef2-Gal4/UAS-dnlg1$^{\Delta N}$;dnlg1−/−* would fail to rescue the synaptic clustering of Dnlg1 and Dnrx, respectively. However, the inability of the C-terminal deletions of these proteins as seen in *elav-Gal4/UAS-Dnrx$^{\Delta c}$;dnrx−/−* and *mef2-Gal4/UAS-dnlg1$^{\Delta C}$;dnlg1−/−* to cluster Dnlg1 and Dnrx, respectively, to wild type localization and/or levels suggest that the lack of the cytoplasmic domains of these proteins

may render the remainder portion of the protein unstable, thereby leading to its inability to be either recruited or held at the synaptic apparatus.

Finally, the subcellular localization of Dlg at the SSR and its levels in the *dnrx* and *dnlg1* single and double mutants as well as in the rescue genotypes (Fig. 3) provides key insights into the stoichiometry of Dnrx-Dnlg1 interactions, and how Dnrx-Dnlg1 might be functioning with other synaptic proteins in their vicinity to organize the synaptic machinery. A significant reduction in Dlg levels in *dnrx* mutants raises the question of whether Dlg localization/levels are controlled presynaptically? Alternatively, it is possible that Dnrx-Dnlg1 is not mutually exclusive for all their synaptic functions and there might be other Neuroligins that might function with Dnrx. One attractive candidate could be Dnlg2, which is both pre- and postsynaptic (Chen et al. 2012). Dnrx could also function through the recently identified Neuroligins 3 and 4 (Xing et al. 2014; Li et al. 2013). Although *dnlg1* mutants did not show any significant difference in Dlg levels, a diffuse subcellular localization nevertheless raised the possibility of a structural disorganization of the postsynaptic terminal and defects in SSR morphology, which were confirmed by ultrastructural studies (Fig. 4). The rescue analysis of the subcellular localization of Dlg demonstrates that Dlg localization and levels could be restored fully in a presynaptic rescue of *dnrx* mutants by expression of full length Dnrx, however the localization of Dlg could not be restored by expression of $Dnrx^{\Delta NT}$ (data not shown). These observations suggest that the extracellular domain of Dnrx is essential for the localization and also the levels of Dlg. Whether the extracellular domain influences Dlg via Dnlg1 or any of the other three Dnlgs (2, 3 and 4) at the NMJ remains to be elucidated.

4.2 Dnrx/Dnlg1 in Wit Stability and Coordination of Synapse Growth

Most studies on Nrx/Nlg across species offer clues as to how these proteins assemble synapses and how they might function in the brain to establish and modify neuronal network properties and cognition, however, very little is known on the signaling pathways that these proteins may potentially function in. It has been previously reported that Neurexin 1 is induced by BMP growth factors *in vitro* and *in vivo* and that could possibly allow regulation of synaptic growth and development (Patzke et al., 2001). In *Drosophila*, both *dnrx* and *dnlg1* mutants showed reduced synaptic growth similar to *wit* pathway mutants (Li et al., 2007; Banovic et al., 2010; McCabe et al., 2002; Aberle et al., 2002; Marques et al., 2003; Merino et al., 2009; Ball et al., 2010). Reduced Wit levels (Fig. 5) both from immunolocalization studies in *dnrx* and *dnlg1* mutant backgrounds and biochemical studies from immunoblot and sucrose density gradient sedimentation analyses present compelling evidence towards the requirement of Dnrx and Dnlg1 for Wit stability. Reduction of synaptic Dnrx levels in *wit* mutants argue for interdependence in the localization of these presynaptic proteins at the NMJ synaptic boutons. Our findings that synaptic boutons of *dnrx* and *dnlg1* mutants also show reduction in the levels of the co-receptor Tkv (Fig. 8) suggest that this effect may not be exclusively Wit-specific, and possibly due to the overall integrity of trans-synaptic adhesion complex that ensures Wit and Tkv stability at the NMJ.

Genetic interaction studies (Fig. 6) displayed a significant reduction in bouton numbers resulting from trans-heterozygous combinations of *wit/+,dnrx/+* and *wit/+,dnlg1/+* compared

to the single heterozygotes strongly favoring the likelihood of these genes functioning together in the same pathway. Although double mutants of *wit,dnrx* and *wit,dnlg1* are somewhat severe than *dnrx* and *dnlg1* single mutants, they did not reveal any significant differences in their bouton counts compared to *wit* single mutants. Moreover, genetic interactions between *Mad;dnrx* and *Mad;dnlg1* together with decreased levels of pMad in *dnrx* and *dnlg1* mutants (Fig. 8) provided further evidence that Dnrx and Dnlg1 regulate components of the BMP pathway. These findings strongly support that *dnrx, dnlg1* and *wit* function cooperatively to coordinate synaptic growth and signaling at the NMJ.

4.3 Dnrx, Dnlg1 and Wit Function in Organizing the Pre- and Postsynaptic Apparatus

Loss of either Dnrx or Dnlg1 does not completely abolish the apposition of pre- and post-synaptic membrane at the NMJ synapses but detachments that occur at multiple sites along the synaptic zone. These observations point to either unique clustering of the Dnlg1/Dnrx molecular complexes or preservation of trans-synaptic adhesion by other adhesion molecules at the NMJ synapses. Indeed, recent studies show nanoscale organization of synaptic adhesion molecules Neurexin 1β, NLG1 and LRRTM2 to form trans-synaptic adhesive structures (Chamma et al. 2016). In addition to *dnrx* and *dnlg1* mutants, synaptic ultrastructural analysis showed similarity in presynaptic membrane detachments with a characteristic ruffling morphology in *wit* mutants as well (Aberle et al. 2002; McCabe et al. 2002) suggesting that these proteins are required for maintaining trans-synaptic adhesion. Interestingly, double mutants from any combinations of these three genes such as *dnlg1,dnrx* (Fig. 4) or *wit,dnrx* and *wit,dnlg1* (Fig. 7) did not show any severity in the detachment/ruffling of the presynaptic membrane suggesting that there might be a phenotypic threshold that cannot be surpassed as part of an intrinsic synaptic machinery to preserve its very structure and function. It would be interesting to test this possibility if more than two genes are lost simultaneously as in a triple mutant combination. Alternatively, there could be presence of other distinct adhesive complexes that remain intact and function outside the realm of Dnrx, Dnlg1 and Wit proteins thus preventing a complete disintegration of the synaptic apparatus.

The same holds true for most of the ultrastructural pre- and postsynaptic differentiation defects observed in the single and double mutants of *dnrx, dnlg1* and *wit*. Barring *dnrx,dnlg1* double mutants in which the SSR width showed a significant reduction compared to the individual single mutants (Fig. 4), all other phenotypes documented from our ultrastructural analysis showed no difference in severity between single and double mutants. Another common theme that emerged from our ultrastructural analysis was that loss of either pre- or postsynaptic proteins or any combinations there of, showed a mixture of defects that spanned both sides of the synaptic terminal. For example, presynaptic phenotypes such as increased number of active zones or abnormally long active zones as well as postsynaptic phenotypes such as reduction in width and density of the SSR were observed when presynaptic proteins such as Dnrx and Wit and postsynaptic Dnlg1 were lost individually or in combination. These studies suggest that pre- and postsynaptic differentiation is tightly regulated and not mutually exclusive where loss of presynaptic proteins would result only in presynaptic deficits and vice-versa.

The postsynaptic SSR phenotypes seen in the single and double mutants of *dnrx, dnlg1* and *wit* might be due to their interaction/association with postsynaptic or perisynaptic protein complexes such as Dlg and Fasciclin II (Thomas et al. 1997). Alternatively, the postsynaptic differentiation or maturation deficits in these mutants could also be due to a failure of postsynaptic GluRs to be localized properly or their levels maintained sufficiently. It has been shown previously that lack of GluR complexes interferes with the formation of SSR (Schmid et al. 2006). Deficits in postsynaptic density assembly have been previously reported for *dnlg1* mutants, including a misalignment of the postsynaptic GluR fields with the presynaptic transmitter release sites (Banovic et al. 2010). GluR distribution also showed profound abnormalities in *dnrx* mutants (Li et al. 2007). These observations suggest that trans-synaptic adhesion and synapse organization and growth is highly coordinated during development, and that multiple molecular complexes may engage in ensuring proper synaptic development. Some of these questions need to be addressed in future investigations.

4.4 Trans-Synaptic Adhesion and Signaling at the NMJ

In *Drosophila*, the postsynaptic muscle-derived BMP ligand, glass bottom boat (Gbb), binds to type II receptor Wit, and type I receptors Tkv, and Saxophone (Sax) at the NMJ (Ball et al. 2010). Receptor activation by Gbb leads to the recruitment and phosphorylation of Mad at the NMJ terminals (schematic in Fig. 8R) followed by nuclear translocation of pMad with the co-Smad, Medea, and transcriptional initiation of other downstream targets (Aberle et al. 2002; Marques et al. 2002; McCabe et al. 2003; Rawson et al. 2003; Ball et al. 2010). It is interesting to note that previously published studies revealed that a postsynaptic signaling event occurs during larval development mediated by Type I receptor Tkv and Mad (Fig. 8R; Dudu et al. 2006). Based on our findings from this study, we speculate that Dnrx and Dnlg1-mediated trans-synaptic adhesive complex allows recruitment and stabilization of Wit and associated components to assemble a larger BMP signaling complex to ensure proper downstream signaling. Loss of Dnrx and/or Dnlg1 results in loss of adhesion and a decrease in the levels of Wit/Tkv receptors as well as decreased phosphorylation of Mad. Thus a combination of trans-synaptic adhesion and signaling mediated by Dnrx, Dnlg1 and components of the BMP pathway orchestrate the assembly of the NMJ and coordinate proper synaptic growth and architecture.

5. Conclusion

The data presented here address fundamental questions of how the interplay of pre- and postsynaptic proteins contributes towards the trans-synaptic adhesion, synapse differentiation and growth during organismal development. Dnrx and Dnlg1 establish trans-synaptic adhesion and functionally associate with the presynaptic signaling receptor Wit to engage as a molecular machinery to coordinate synaptic growth, cytoarchitecture and signaling. Dnrx and Dnlg1 also function in regulating BMP receptor levels (Wit and Tkv) as well as the downstream effector, Mad, at the NMJ. It is thus conceivable that at the molecular level setting up of a Dnrx-Dnlg1 mediated trans-synaptic adhesion is a critical component for molecules such as Wit and Tkv to perform signaling function. It would be of immense interest to investigate how mammalian Neurexins and Neuroligins are engaged with signaling pathways that not only are involved in synapse formation but also their

functional modulation, as the respective genetic loci show strong associations with cognitive and neurodevelopmental disorders.

Supplementary Material

Refer to Web version on PubMed Central for supplementary material.

Acknowledgments

We thank H. Aberle, H. Bellen, V. Budnik, Y. Cai, A. DiAntonio, B. Eaton, M. Gonzalez-Gaitan, L. Griffith, P. Haghighi, J. Han, B. McCabe, B. Mozer, M. O'Connor, and S. Sigrist for generously sharing their reagents. We thank B. Eaton and members of the Bhat laboratory for helpful discussions and M. Riordan and C. Burch for technical assistance. This work was supported by grants from the Simons Foundation Autism Research Initiative (SFARI-177037), the National Institutes of Health (NS050356), the Zachry Foundation and the University of Texas Health Science Center, San Antonio.

References

Aberle H, Haghighi AP, Fetter RD, McCabe BD, Magalhaes TR, Goodman CS. wishful thinking encodes a BMP type II receptor that regulates synaptic growth in Drosophila. Neuron. 2002; 33:545–558. [PubMed: 11856529]

Aoto J, Foldy C, Ilcus SM, Tabuchi K, Sudhof TC. Distinct cirucuit-dependent functions of presynaptic neurexin-3 at GABAergic and glutamatergic synapses. Nat Neuroscience. 2015; 18:997–1007. [PubMed: 26030848]

Ashley J, Packard M, Ataman B, Budnik V. Fasciclin II signals new synapse formation through amyloid precursor protein and scaffolding protein dX11/Mint. J Neurosci. 2005; 25:5943–5955. [PubMed: 15976083]

Ball RW, Warren-Paquin M, Tsurudome K, Liao EH, Elazzouzi F, Cavanagh C, An BS, Wang TT, White JH, Haghighi AP. Retrograde BMP signaling controls synaptic growth at the NMJ by regulating trio expression in motor neurons. Neuron. 2010; 66:536–549. [PubMed: 20510858]

Banerjee S, Riordan M, Bhat MA. Genetic aspects of autism spectrum disorders: insights from animal models. Frontiers in cellular neuroscience. 2014; 8:58. [PubMed: 24605088]

Banerjee S, Pillai AM, Paik R, Li J, Bhat MA. Axonal ensheathment and septate junction formation in the peripheral nervous system of Drosophila. The Journal of neuroscience : the official journal of the Society for Neuroscience. 2006; 26:3319–3329. [PubMed: 16554482]

Banovic D, Khorramshahi O, Owald D, Wichmann C, Riedt T, Fouquet W, Tian R, Sigrist SJ, Aberle H. Drosophila neuroligin 1 promotes growth and postsynaptic differentiation at glutamatergic neuromuscular junctions. Neuron. 2010; 66:724–738. [PubMed: 20547130]

Berke B, Wittnam J, McNeill E, Van Vactor DL, Keshishian H. Retrograde BMP signaling at the synapse: a permissive signal for synapse maturation and activity-dependent plasticity. Journal of neuroscience. 2013; 33:17937–17950. [PubMed: 24198381]

Budnik V, Koh YH, Guan B, Hartmann B, Hough C, Woods D, Gorczyca M. Regulation of synapse structure and function by the Drosophila tumor suppressor gene dlg. Neuron. 1996; 17:627–640. [PubMed: 8893021]

Chen YC, Lin YQ, Banerjee S, Venken K, Li J, Ismat A, Chen K, Duraine L, Bellen HJ, Bhat MA. Drosophila neuroligin 2 is required presynaptically and postsynaptically for proper synaptic differentiation and synaptic transmission. The Journal of neuroscience : the official journal of the Society for Neuroscience. 2012; 32:16018–16030. [PubMed: 23136438]

Chih B, Engleman H, Scheiffele P. Control of excitatory and inhibitory synapse formation by neuroligins. Science. 2005; 307:1324–1328. [PubMed: 15681343]

Chamma I, Letellier M, Butler C, Tessier B, Lim KH, Gauthereau I, Choquet D, Sibarita JB, Park S, Sainlos M, Thoumine O. Mapping the dynamics and nanoscale organization of synaptic adhesion proteins using monomeric streptavidin. Nature Commun. 2016; 7:10773. [PubMed: 26979420]

Chubykin AA, Atasoy D, Etherton MR, Brose N, Kavalali ET, Gibson JR, Sudhof TC. Activity-dependent validation of excitatory versus inhibitory synapses by neuroligin-1 versus neuroligin-2. Neuron. 2007; 54:919–931. [PubMed: 17582332]

Dudu V, Bittig T, Entchev E, Kicheva A, Jülicher F, González-Gaitán M. Postsynaptic mad signaling at the Drosophila neuromuscular junction. Curr Biol. 2006; 16:625–635. [PubMed: 16581507]

Eaton BA, Fetter RD, Davis GW. Dynactin is necessary for synapse stabilization. Neuron. 2002; 34:729–741. [PubMed: 12062020]

Graf ER, Zhang X, Jin SX, Linhoff MW, Craig AM. Neurexins induce differentiation of GABA and glutamate postsynaptic specializations via neuroligins. Cell. 2004; 119:1013–1026. [PubMed: 15620359]

Ichtchenko K, Hata Y, Nguyen T, Ullrich B, Missler M, Moomaw C, Sudhof TC. Neuroligin 1: a splice site-specific ligand for beta-neurexins. Cell. 1995; 81:435–443. [PubMed: 7736595]

Lahey T, Gorczyca M, Jia XX, Budnik V. The Drosophila tumor suppressor gene dlg is required for normal synaptic bouton structure. Neuron. 1996; 13:823–835.

Li J, Ashley J, Budnik V, Bhat MA. Crucial role of Drosophila neurexin in proper active zone apposition to postsynaptic densities, synaptic growth, and synaptic transmission. Neuron. 2007; 55:741–755. [PubMed: 17785181]

Marques G, Bao H, Haerry TE, Shimell MJ, Duchek P, Zhang B, O'Connor MB. The Drosophila BMP type II receptor Wishful Thinking regulates neuromuscular synapse morphology and function. Neuron. 2002; 33:529–543. [PubMed: 11856528]

McCabe BD, Marques G, Haghighi AP, Fetter RD, Crotty ML, Haerry TE, Goodman CS, O'Connor MB. The BMP homolog Gbb provides a retrograde signal that regulates synaptic growth at the Drosophila neuromuscular junction. Neuron. 2003; 39:241–254. [PubMed: 12873382]

Merino C, Penney J, Gonzalez M, Tsurudome K, Moujahidine M, O'Connor MB, Verheyen EM, Haghighi P. Nemo kinase interacts with Mad to coordinate synaptic growth at the Drosophila neuromuscular junction. The Journal of cell biology. 2009; 185:713–725. [PubMed: 19451277]

Missler M, Zhang W, Rohlmann A, Kattenstroth G, Hammer RE, Gottmann K, Sudhof TC. Alpha-neurexins couple Ca2+ channels to synaptic vesicle exocytosis. Nature. 2003; 423:939–948. [PubMed: 12827191]

Mozer BA, Sandstrom DJ. Drosophila neuroligin 1 regulates synaptic growth and function in response to activity and phosphoinositide-3-kinase. Molecular and cellular neurosciences. 2012; 51:89–100. [PubMed: 22954894]

Nahm M, Lee MJ, Parkinson W, Lee M, Kim H, Kim YJ, Kim S, Cho YS, Min BM, Bae YC, Broadie K, Lee S. Spartin regulates synaptic growth and neuronal survival by inhibiting BMP-mediated microtubule stabilization. Neuron. 2013; 77:680–695. [PubMed: 23439121]

Patzke H, Reissmann E, Stanke M, Bixby JL, Ernsberger U. BMP growth factors and Phox2 transcription factors can induce synaptotagmin I and neurexin I during sympathetic neuron development. Mech Dev. 2001; 108:149–159. [PubMed: 11578868]

Pielage J, Fetter RD, Davis GW. Presynaptic spectrin is essential for synapse stabilization. Curr Biol. 2005; 15:918–928. [PubMed: 15916948]

Prange O, Wong TP, Gerrow K, Wang YT, El-Husseini A. A balance between excitatory and inhibitory synapses is controlled by PSD-95 and neuroligin. Proc Natl Acad Sci USA. 2004; 101:13915–13920. [PubMed: 15358863]

Rawson JM, Lee M, Kennedy EL, Selleck SB. Drosophila neuromuscular synapse assembly and function require the TGF-beta type I receptor saxophone and the transcription factor Mad. J Neurobiol. 2003; 55:134–150. [PubMed: 12672013]

Rothwell PE, Fuccillo MV, Maxeiner S, Hayton SJ, Gokce O, Lim BK, Fowler SC, Malenka RC, Sudhof TC. Autism-associated neuroligin-3 mutations commonly impair striatal circuits to boost repetitive behaviors. Cell. 2014; 158:198–212. [PubMed: 24995986]

Scheiffele P, Fan J, Choih J, Fetter R, Serafini T. Neuroligin expressed in nonneuronal cells triggers presynaptic development in contacting axons. Cell. 2000; 101:657–669. [PubMed: 10892652]

Schmid A, Qin G, Wichmann C, Kittel RJ, Mertel S, Fouquet W, Schmidt M, Heckmann M, Sigrist SJ. Non-NMDA-type glutamate receptors are essential for maturation but not for initial assembly at Drosophila neuromuscular junctions. J. Neurosci. 2006; 26:11267–11277. [PubMed: 17079654]

Song JY, Ichtchenko K, Sudhof TC, Brose N. Neuroligin 1 is a postsynaptic cell-adhesion molecule of excitatory synapses. Proceedings of the National Academy of Sciences of the United States of America. 1999; 96:1100–1105. [PubMed: 9927700]

Sudhof TC. Neuroligins and neurexins link synaptic function to cognitive disease. Nature. 2008; 455:903–911. [PubMed: 18923512]

Sulkowski M, Kim YJ, Serpe M. Postsynaptic glutamate receptors regulate local BMP signaling at the Drosophila neuromuscular junction. Development. 2014; 141:436–447. [PubMed: 24353060]

Thomas U, Kim E, Kuhlendahl S, Koh YH, Gundelfinger ED, Sheng M, Garner CC, Budnik V. Synaptic clustering of the cell adhesion molecule fasciclin II by discs-large and its role in the regulation of presyantpic structure. Neuron. 1997; 19:787–799. [PubMed: 9354326]

Tian Y, Li T, Sun M, Wan D, Li Q, Li P, Zhang ZC, Han J, Xie W. Neurexin regulates visual function via mediating retinoid transport to promote rhodopsin maturation. Neuron. 2013; 77:311–322. [PubMed: 23352167]

Ushkaryov YA, Petrenko AG, Geppert M, Sudhof TC. Neurexins: synaptic cell surface proteins related to the alpha-latrotoxin receptor and laminin. Science. 1992; 257:50–56. [PubMed: 1621094]

Varoqueaux F, Aramuni G, Rawson RL, Mohrmann R, Missler M, Gottmann K, Zhang W, Sudhof TC, Brose N. Neuroligins determine synapse maturation and function. Neuron. 2006; 51:741–754. [PubMed: 16982420]

Wagh DA, Rasse TM, Asan E, Hofbauer A, Schwenkert I, Durrbeck H, Buchner S, Dabauvalle MC, Schmidt M, Qin G, Wichmann C, Kittel R, Sigrist SJ, Buchner E. Bruchpilot, a protein with homology to ELKS/CAST, is required for structural integrity and function of synaptic active zones in Drosophila. Neuron. 2006; 49:833–844. [PubMed: 16543132]

Wittenmayer N, Korber C, Liu H, Kremer T, Varoqueaux F, Chapman ER, Brose N, Kuner T, Dresbach T. Postsynaptic Neuroligin1 regulates presynaptic maturation. Proceedings of the National Academy of Sciences of the United States of America. 2009; 106:13564–13569. [PubMed: 19628693]

Xing G, Gan G, Chen D, Sun M, Yi J, Lv H, Han J, Xie W. Drosophila neuroligin 3 regulates neuromuscular junction development and synaptic differentiation. J. Biol Chem. 2014; 289:31867–31877. [PubMed: 25228693]

Zhang B, Chen LY, Liu X, Maxeiner S, Lee SJ, Gokce O, Sudhof TC. Neuroligins scuplt cerebellar purkinje-cell circuits by differential control of distinct classes of synapses. Neuron. 2015; 87:781–796. [PubMed: 26291161]

Highlights

- *Drosophila neurexin* and *neuroligin 1* display genetic and biochemical interactions.
- Dnrx and Dnlg1 are required for subcellular localization of Dlg at the synapse.
- Dnrx and Dnlg1 are required for the localization and stability of BMP receptor Wit.
- Dnrx and Dnlg1 regulate levels of BMP co-receptor Tkv and downstream effector Mad.
- Proper trans-synaptic adhesion is crucial for BMP receptor stability and signaling.

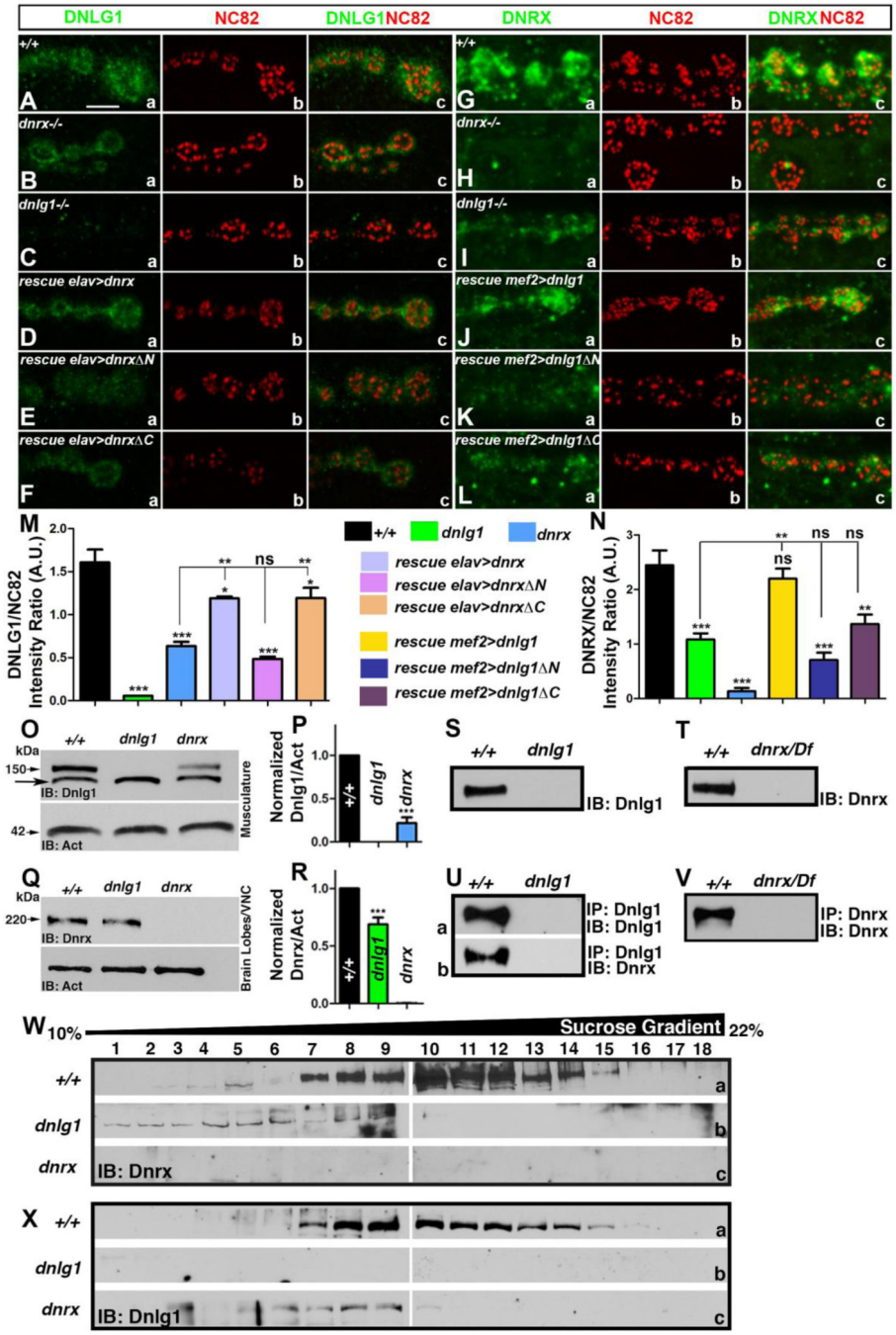

Figure 1. Interdependence in synaptic clustering of Dnlg1 and Dnrx

(A-L) Confocal micrograhs of 3rd instar larval NMJ labeled with antibodies against Dnlg1 (A-F, green), Dnrx (G-L, green) and active zone protein Bruchpilot (NC82, red, A-L). Scale bar equals 5μM for panels (A-L).

(M, N) Quantification of Dnlg1/NC82 (M) and Dnrx/NC82 (N) fluorescence intensity ratio in the specified genotypes. Number of larvae (n) for each genotype under different experimental group was 8.

(O) Immunoblots of larval musculature extracts from wild type, *dnlg1* and *dnrx* mutants probed with anti-Dnlg1 (O, arrowhead, 150kDa) showing levels of Dnlg1. Arrow points to a non-specific band in the Dnlg1 immunoblot. Anti-Actin was used as a protein loading control (arrow, 42kDa).

(Q) Immunoblots from 3rd instar larval brain lobe/VNC extracts showing levels of Dnrx (Q, arrow, 220kDa) in wild type, *dnlg1* and *dnrx* mutants.

(P, R) Quantification of the ratio of band intensities of Dnlg1 (P) and Dnrx (R) with their respective Actin levels used as loading control.

(S-V) Adult head lysates of wild type (+/+) and *dnlg1* probed with anti-Dnlg1 (S), and wild type (+/+) and *dnrx/Df* probed with anti-Dnrx (T) antibodies. Head lysates of wild type (+/+) in combination with either *dnlg1* or *dnrx/Df* immunoprecipitated with anti-Dnlg1 (Ua, b) and anti-Dnrx (V).

(W, X) 10–45% continuous sucrose density gradient centrifugation of head lysates from the wild type, *dnrx* and *dnlg1* mutants immunoblotted against Dnrx (W) and Dnlg1 (X) show Dnrx and Dnlg1 in overlapping fractions (7–15) in wild type (+/+, compare Wa and Xa). Gradient fractions that correspond up to ~22% sucrose are shown.

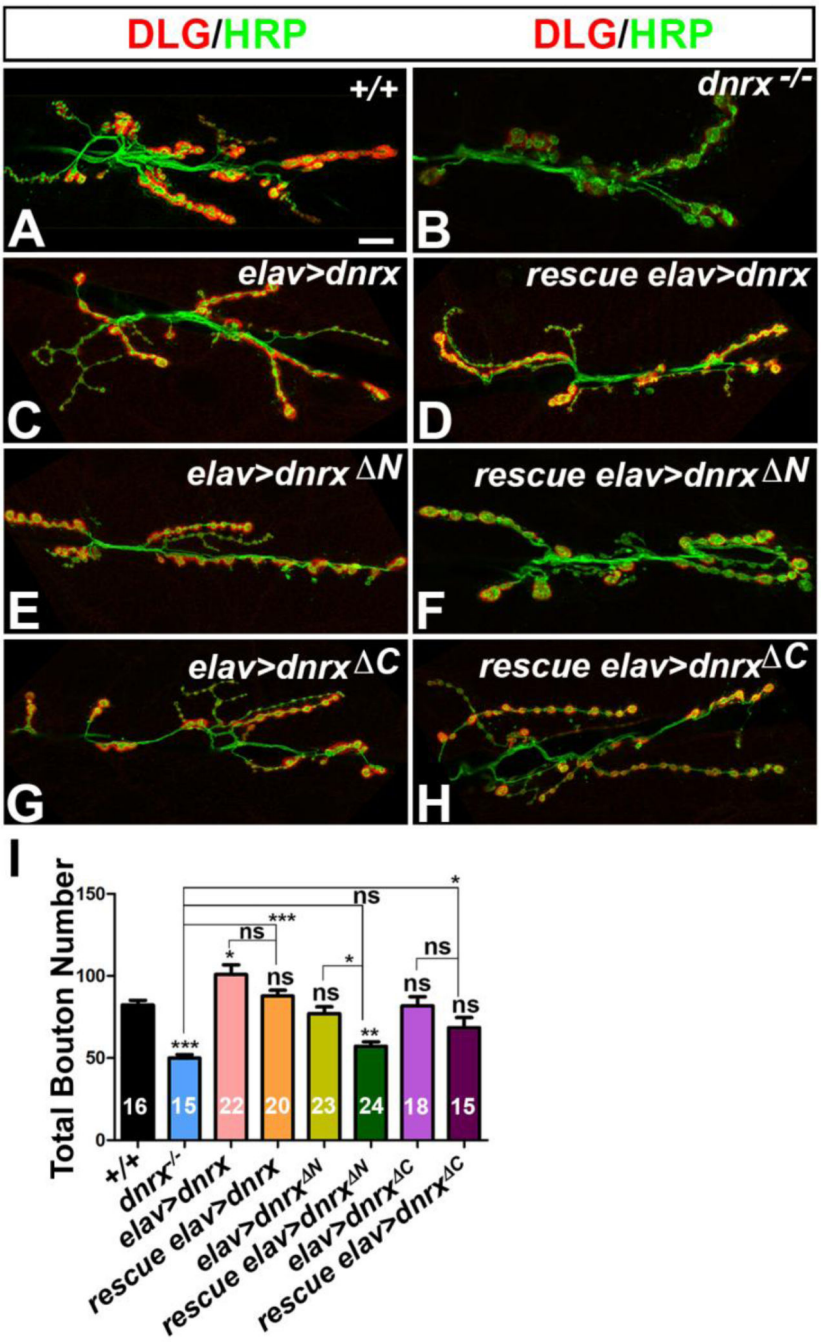

Figure 2. Domain-specific requirement of Dnrx in synaptic growth

(A-H) Merged confocal sections from 3rd instar larval NMJ of muscle 6/7 immunostained with antibodies against the presynaptic marker Hrp (green) and the postsynaptic marker Dlg (red) show synaptic growth in wild type (+/+, A), *dnrx* (B), presynaptic overexpression of Dnrx (C), Dnrx$^{\Delta N}$ (E) and Dnrx$^{\Delta C}$ (G) using *elav-Gal4* in the wild type background. Corresponding *dnrx* mutant rescues using presynaptic overexpression of Dnrx (D), Dnrx$^{\Delta N}$ (F) and Dnrx$^{\Delta C}$ (H). (I) Quantification of total bouton numbers in indicated genotypes.

Number of larvae quantified (n) for each genotype is indicated within the bar. Scale bar: 10μM.

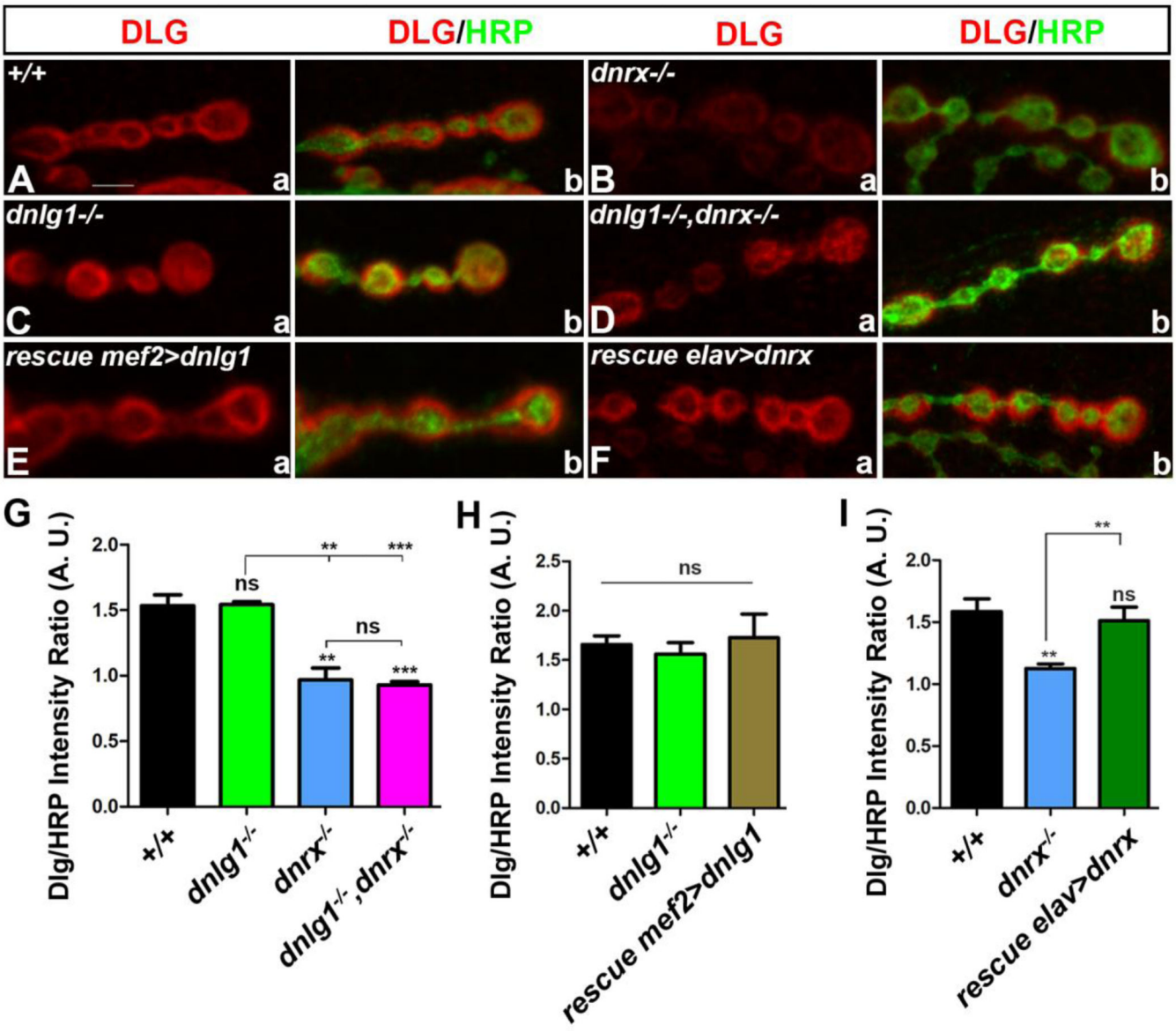

Figure 3. Subcellular localization of Dlg is altered in single and double mutants of *dnlg1* and *dnrx*

(A-F) Representative confocal images of NMJ boutons double-stained with anti-Dlg (red) and anti-Hrp (green) antibodies. Dlg localization in wild type (+/+, Aa,b) boutons is concentrated at the SSR. Dlg levels are significantly reduced in *dnrx* (Ba,b), and display a uniform distribution in *dnlg1* (Ca,b) compared to wild type (A). Double mutants of *dnlg1,dnrx* show reduction in levels of Dlg (Da,b) and a uniform distribution. Dlg localization is rescued when full length Dnlg1 is expressed postsynaptically using *mef2-Gal4* (Ea, b). Dlg levels also get restored in *dnrx* mutants upon overexpression of full length Dnrx presynaptically using *elav-Gal4* (Fa,b).

(G-I) Quantification of Dlg/Hrp fluorescence intensity ratio in the specified genotypes. Number of larvae (n) for each genotype under different experimental group was 8.

Scale bar: 5μM.

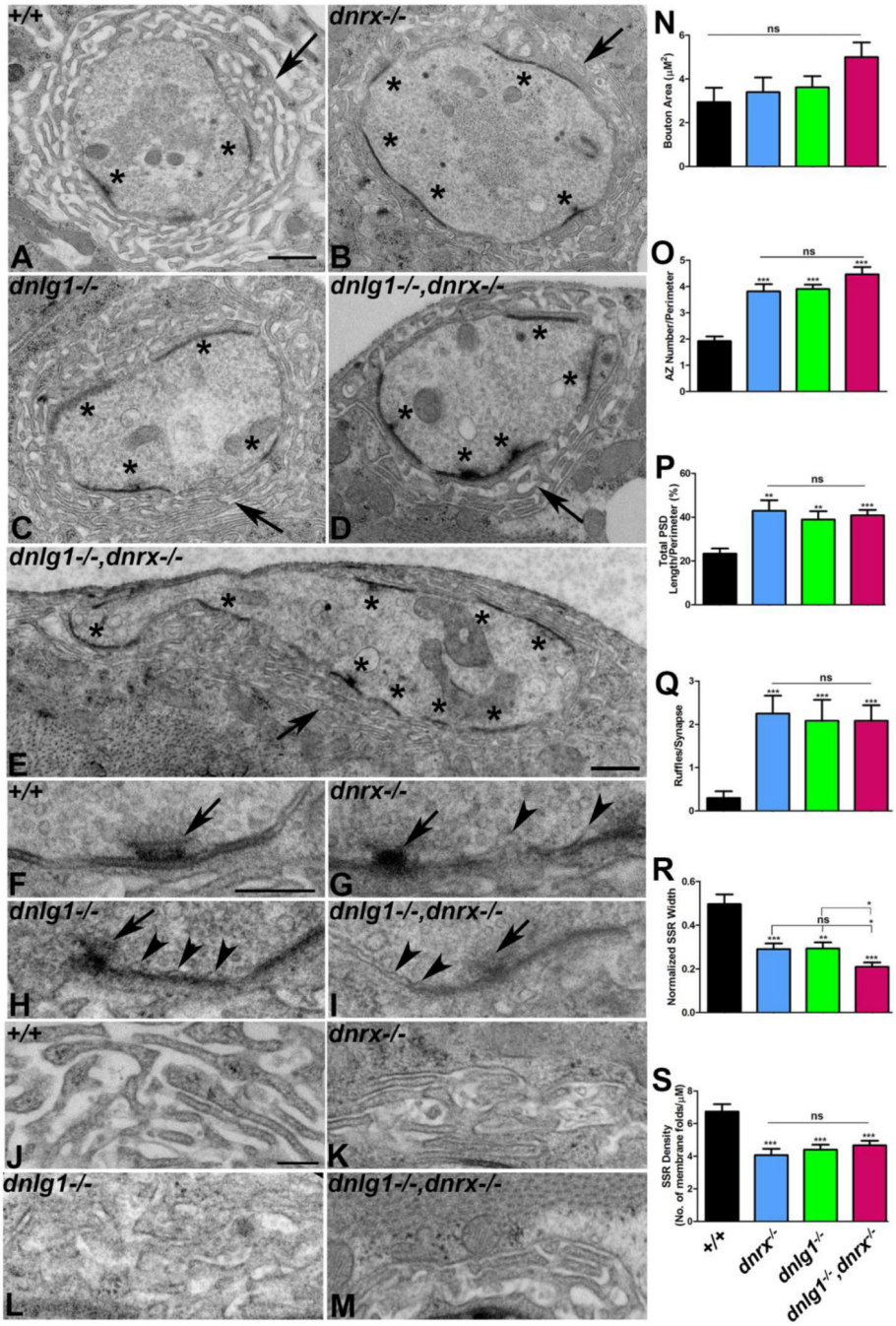

Figure 4. Synaptic ultrastructure is altered in *dnrx* and *dnlg1* single and double mutants

(A-D) Ultrastructure of type Ib synaptic boutons in wild type (+/+, A), *dnrx* (B), *dnlg1* (C) and *dnlg1,dnrx* (D). Note the abundant clear vesicles, electron dense active zones (asterisks), and the SSR localized around the presynaptic bouton (arrow) in wild type control (+/+, A). Ultrastructure of mutant type Ib boutons in *dnrx* (B), *dnlg1* (C) and *dnlg1,dnrx* (D) frequently display gross morphological defects that include increase in active zone number (asterisks) and length, and reduced thickness and altered SSR morphology (arrow).

(E) A giant synaptic bouton in *dnrx,dnlg1* that is elongated laterally and have multiple active zones (asterisk) along the perimeter.

(F-I) Higher magnification images show morphology of T-bars (arrow) and a tightly apposed pre- and postsynaptic membrane in wild type (+/+, F). A compromised T-bar together with increasingly detached presynaptic membrane with characteristic ruffles (arrowheads) are observed in *dnrx* (G), *dnlg1* (H) and *dnrx,dnlg1* (I).

(J-M) Higher magnification shows SSR morphology in wild type (+/+, J). Altered SSR morphology that display reduced width, thinner folds, less complexity and convolution is seen in *dnrx* (K), *dnlg1* (L) and *dnlg1,dnrx* (M).

(N-S) Quantification of a variety of pre- and postsynaptic abnormalities including bouton area (N), number of active zone/bouton perimeter (O), total PSD length/bouton perimeter (P), number of membrane ruffles/synapse (Q), normalized SSR width (R) and density of SSR membrane folds/μM (S) are shown in indicated genotypes.

Scale bar for (A-E) equals 600nm and (F-M) equals 200nm.

Number of synaptic boutons (n) from three larvae of each genotype were quantified for morphometric analyses: In *wild type* (n=15), *dnrx* (n=16), *dnlg1* (n=21) and *dnlg1,dnrx* (n=17).

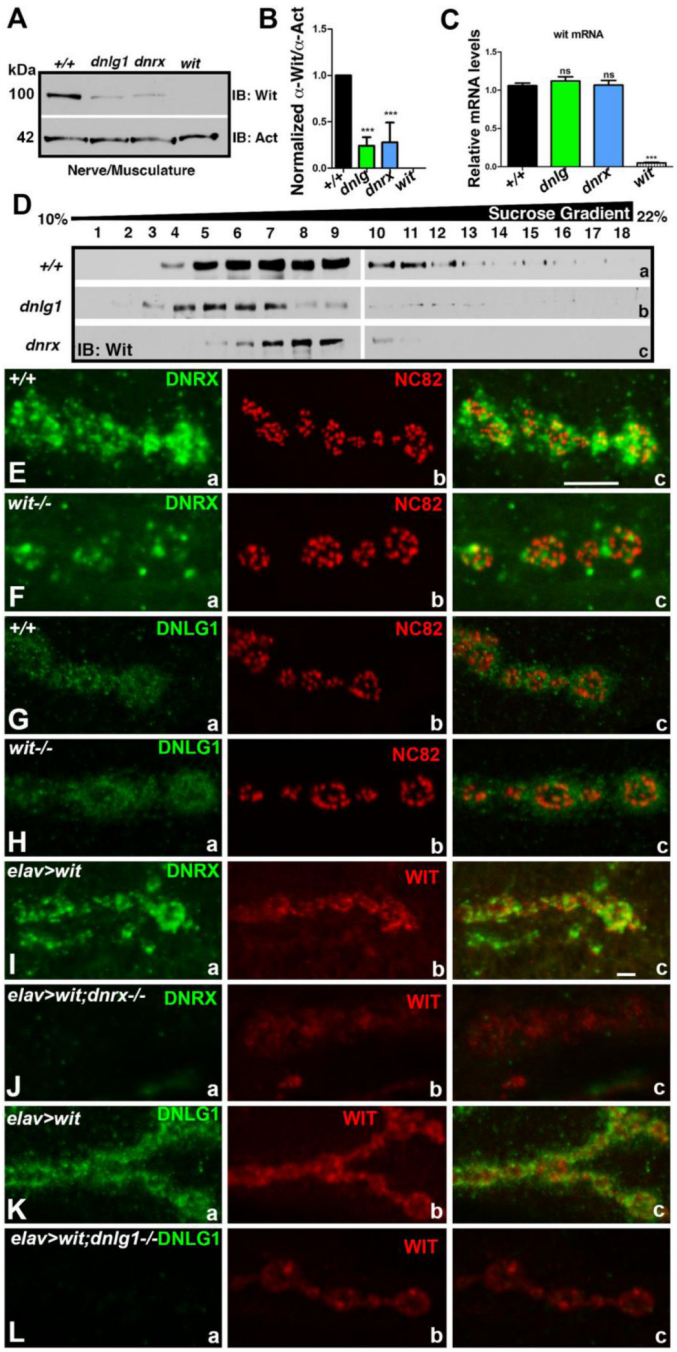

Figure 5. Wit localization and stability is dependent on Dnrx and Dnlg1

(A-D) Immunoblots of larval musculature extracts from wild type (+/+), *dnlg1, dnrx* and *wit* mutants probed with anti-Wit antibodies (100kDa, A) showing levels of Wit. Anti-Actin was used as a protein loading control. Quantification of the ratio of band intensities of Wit with respect to Actin levels as shown in specified genotypes (B). qRTPCR analysis of *wit* mRNA levels in indicated genotypes (C). Sucrose density gradient centrifugation of head lysates from the wild type, *dnrx* and *dnlg1* mutants immunoblotted against Wit (D) show Wit

distribution in fractions (4–15) in wild type (+/+, Da). A decrease in Wit levels and shift in its distribution is observed in *dnlg1* (Db) and *dnrx/Df* (Dc) gradient fractions.
(E, F) 3rd instar larval NMJ of wild type (+/+, E) and *wit* (F) show localization of Dnrx (Ea,c and Fa,c) and NC82 (Eb,c and Fb,c).
(G, H) 3rd instar larval NMJ of wild type (+/+, G) and *wit* (H) co-stained with anti-Dnlg1 (Ga,c and Ha,c) and anti-BRP (NC82, Eb,c and Fb,c).
(I-L) NMJ of *elav-Gal4; UAS-wit* (I, K) show Wit localization (Ib,c and Kb,c) with respect to Dnrx (Ia,c) and Dnlg1 (Ka,c). NMJ of *elav-Gal4; UAS-wit;dnrx−/−* (J) and *elav-Gal4;UASwit;dnlg1−/−* (L) show significant reduction in Wit levels (Jb,c and Lb,c) both in *dnrx* and *dnlg1* mutant backgrounds, respectively.
Scale bar equals 5μM (E-L).

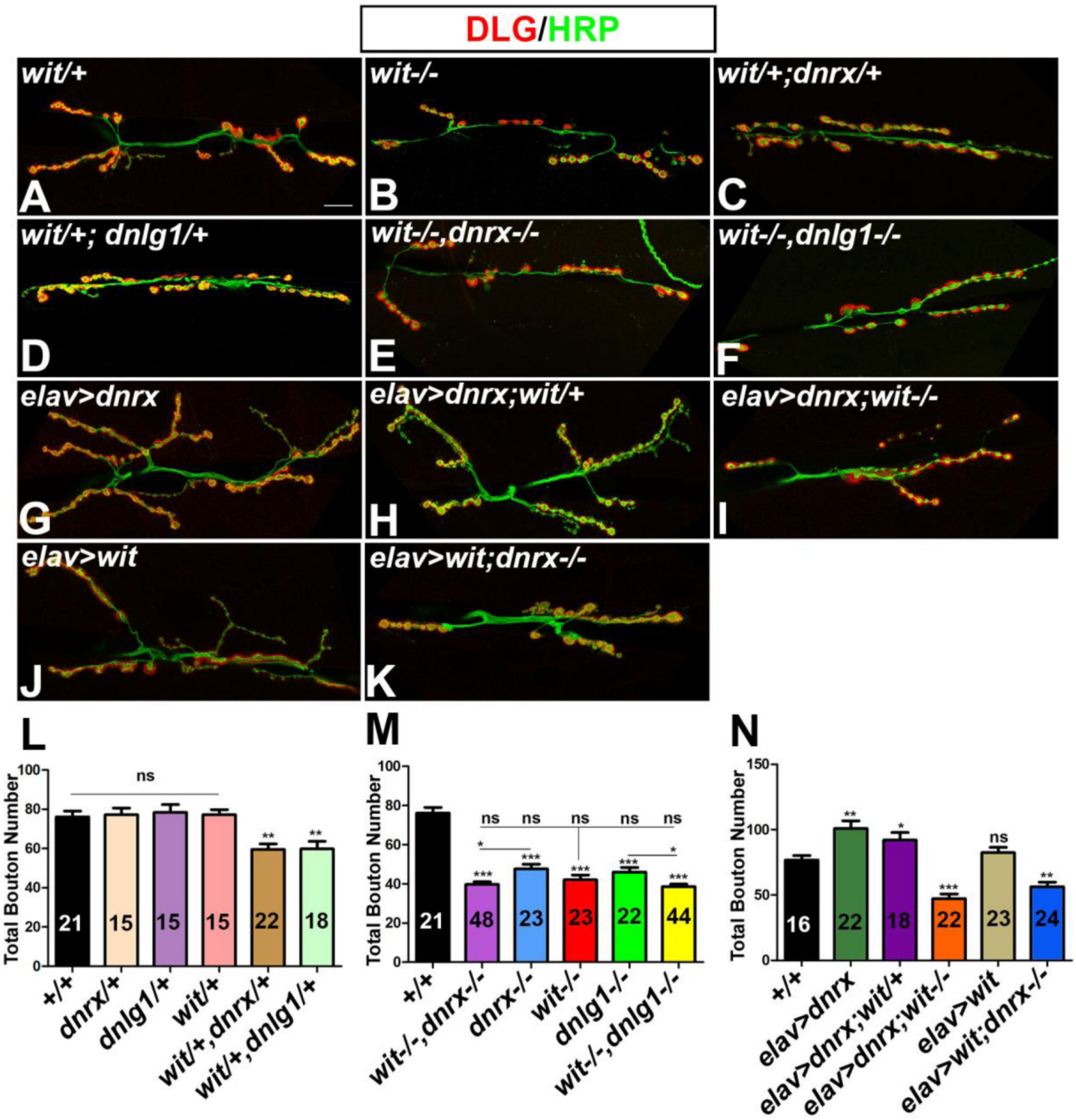

Figure 6. Genetic interactions between *wit,dnrx* and *wit,dnlg1*

(A-K) Confocal micrograph of 3rd instar larval NMJ labeled with anti-Hrp (green) and anti-Dlg (red) show reduced synaptic growth in single mutants of *wit* (B), trans-heterozygotes of *wit,dnrx* (C) and *wit,dnlg1* (D), and double mutants of *wit,dnrx* (E) and *wit,dnlg1* (F) compared to *wit/+* heterozygotes (A).

(G-K) Overgrowth of NMJ boutons caused by presynaptic overexpression of Dnrx (G) is not suppressed by loss of one copy of *wit* (H). Overgrowth phenotype resulting from presynaptic Dnrx overexpression is attenuated by loss of both copies of *wit* (I) and resembles the *wit*

mutant phenotype (B). Presynaptic overexpression of Wit does not cause overgrowth of NMJ boutons (J) and fails to rescue the synaptic undergrowth phenotype of *dnrx* (K).
(L-N) Quantification of the NMJ bouton number at A3 in muscles 6 and 7 of designated genotypes. Number of larvae quantified (n) is indicated within the bars representing various genotypic combinations.
Scale bar equals 10μM.

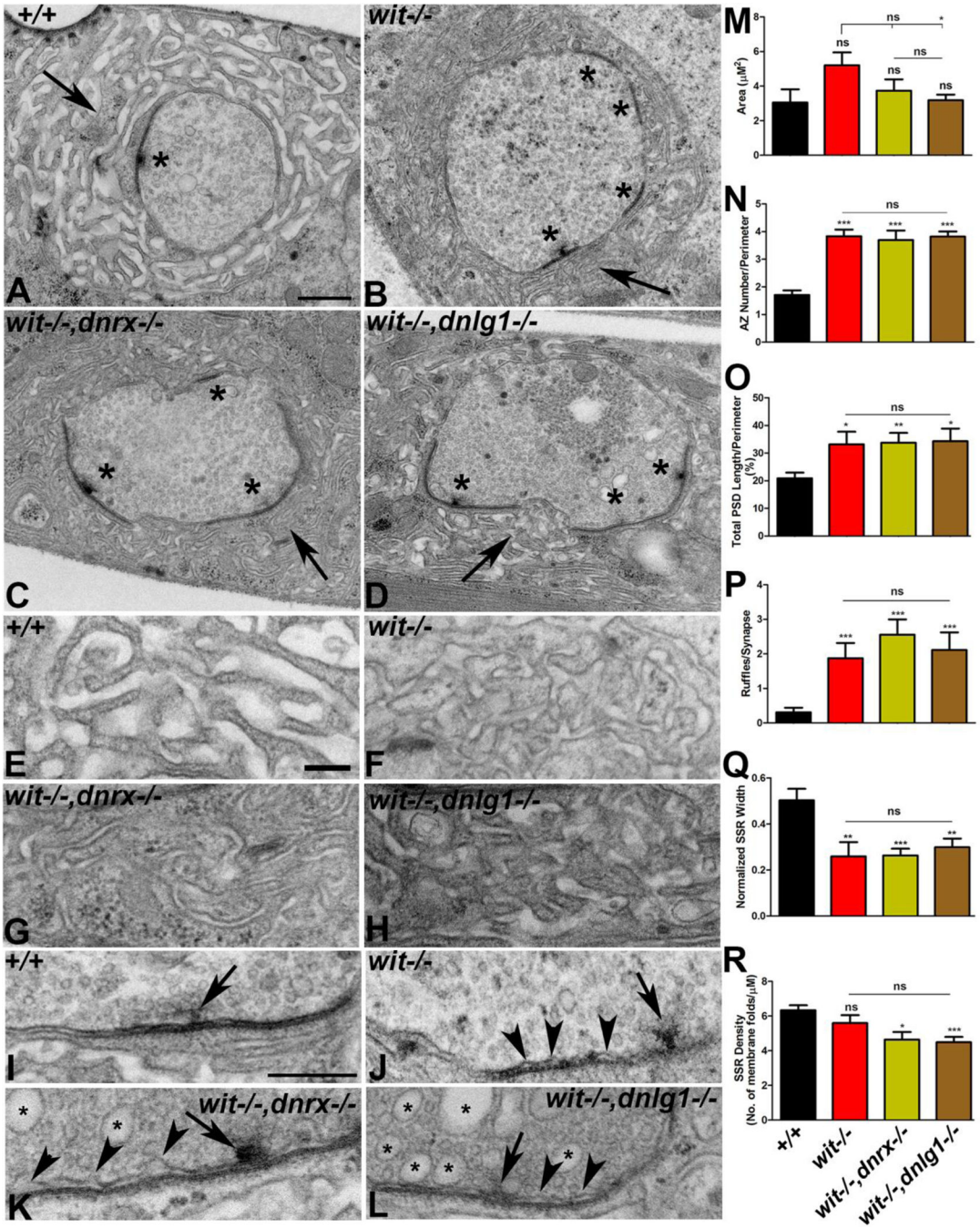

Figure 7. Pre- and postsynaptic abnormalities resulting from individual loss of *wit* and it's combined loss with *dnrx* and *dnlg1*

(A-D) Low magnification TEM images of wild type (+/+, A), *wit* (B), *wit,dnrx* (C) and *wit,dnlg1* (D). Ultrastructure of mutant boutons (B-D) show severely altered SSR morphology (arrows), decreased SSR width, increased PSD length, and increased number of active zones (asterisks) compared to *wild type* (+/+, A).

(E-H) Higher magnification ultrastructural images highlighting the SSR morphology of wild type (+/+, E), *wit* (F), *wit,dnrx* (G) and *wit,dnlg1* (H).

(I-L) Electron micrograph showing pre- and postsynaptic membrane and T-bar (arrow) morphology in wild type (+/+, I), *wit* (J), *wit,dnrx* (K) and *wit,dnlg1* (L). Note the presence of presynaptic membrane ruffles in mutants (arrowheads, J-L) and large synaptic vesicles (arrows) in double mutants of *wit,dnrx* (K) and *wit,dnlg1* (L).
(M-R) Quantification of bouton area (M), number of active zone/perimeter (N), total PSD length/perimeter (O), number of membrane ruffles/synapse (P), normalized SSR width (Q) and density of SSR membrane folds/μM (R) as shown in specified genotypes.
Scale bar for (A-D) equals 600nm and (E-L) equals 200nm.

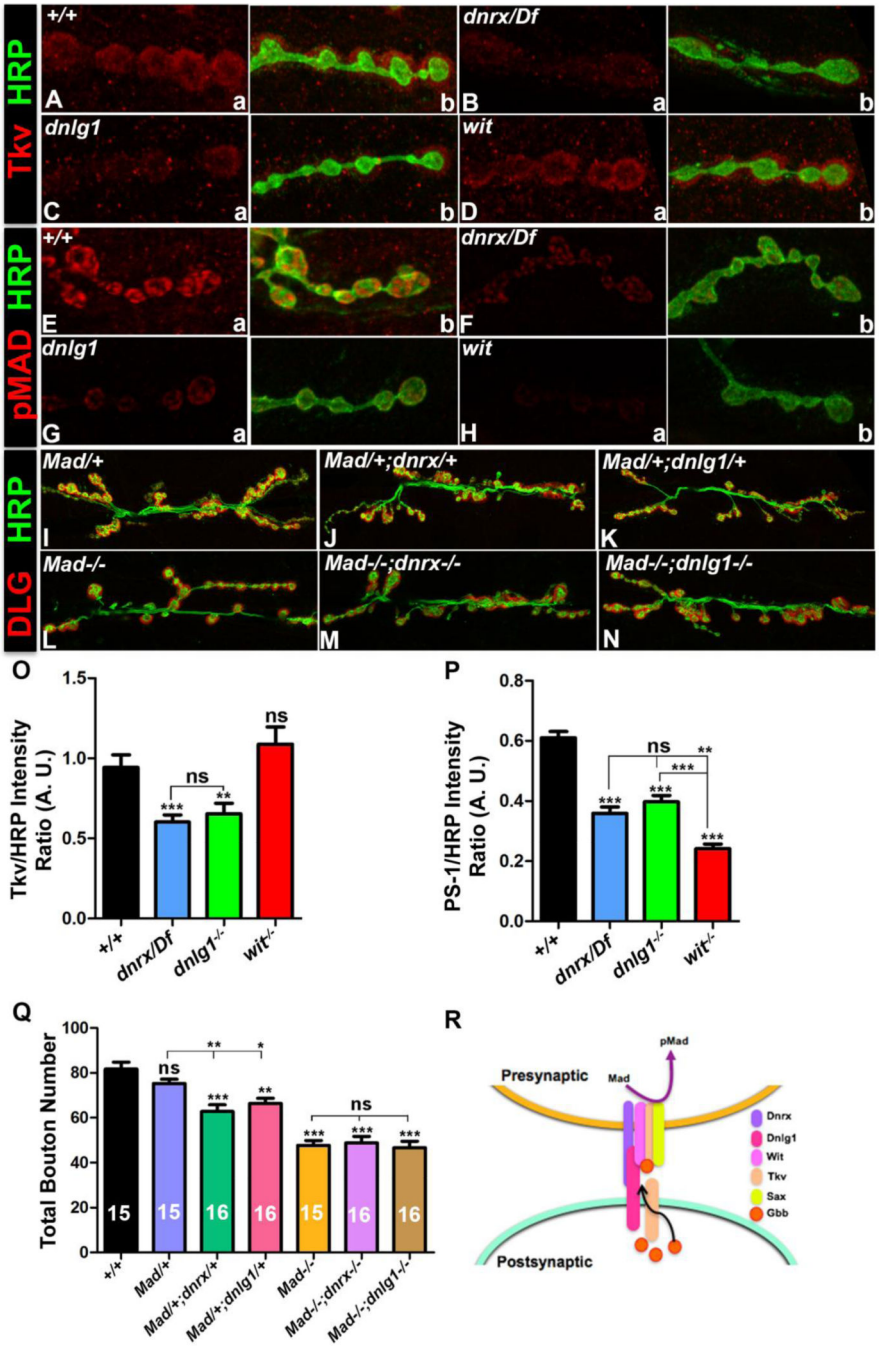

Figure 8. Thick Veins and pMad levels are reduced at *dnrx* and *dnlg1* mutant NMJ synapses

(A-D) Confocal images of NMJ boutons co-labeled with anti-Tkv (red) and anti-Hrp (green) antibodies. Tkv localization in wild type boutons (+/+, Aa,b), *dnrx/Df* (Ba,b), *dnlg1* (Ca,b) and *wit* (Da,b)..

(E-H) Confocal images of NMJ boutons co-labeled with anti-pMad (red) and anti-Hrp (green) in wild type (+/+, Ea,b), *dnrx/Df* (Fa,b), *dnlg1* (Ga,b) and *wit* (Ha,b)..

(I-N) Confocal micrographs of 3rd instar larval NMJ labeled with anti-Hrp (green) and anti-Dlg (red) showing synaptic growth in *Mad/+* (I), double-heterozygotes of *Mad;dnrx* (J), *Mad;dnlg1* (K), $Mad^{-/-}$ (L), and double mutants of *Mad;dnrx* (M) and *Mad;dnlg1* (N).
(O-Q) Quantification of Tkv/Hrp (O) and pMad/Hrp (P) fluorescence intensity ratio in the specified genotypes. Number of larvae (n) analyzed for each genotype was 8.
Number of synaptic boutons (Q) in stated genotypes. Number of larvae quantified (n) is indicated within the bars representing various genotypic combinations.
(R) A model depicting the interactions between Dnrx and Dnlg1 with various components of the BMP signaling pathway at the trans-synaptic interface of NMJ. Optimal BMP signaling requires proper trans-synaptic adhesion and stability of various BMP receptors to guarantee coordinated synaptic growth at the NMJ during development.